NUMERICAL SOLUTIONS OF PARTIAL DIFFERENTIAL EQUATION WITH VARIABLE SPACE OPERATOR AND ITS APPLICATIONS

by

Abdullah Said ERDOĞAN

May 2007

NUMERICAL SOLUTIONS OF PARTIAL DIFFERENTIAL EQUATION WITH VARIABLE SPACE OPERATOR AND ITS APPLICATIONS

by

Abdullah Said ERDOĞAN

A thesis submitted to

the Graduate Institute of Sciences and Engineering

of

Fatih University

in partial fulfillment of the requirements for the degree of

Master of Science

in

Mathematics

May 2007
Istanbul,Turkey

APPROVAL PAGE

I certify that this thesis satisfies all the requirements as a thesis for the degree of Master of Science.

Prof. Dr. Hakkı İsmail ERDOĞAN
Head of Department

This is to certify that I have read this thesis and that in my opinion it is fully adequate, in scope and quality, as a thesis for the degree of Master of Science.

Prof. Dr. Allaberen ASHYRALYEV
Supervisor

Assist. Prof. Dr. Nurullah ARSLAN
Supervisor

Examining Committee Members

Prof. Dr. Allaberen ASHYRALYEV

Prof. Dr. Mustafa BAYRAM

Assc. Prof. Dr. Alexey LUKASHOV

Assist. Prof. Dr. Nurullah ARSLAN

Assist. Prof. Dr. İbrahim KARATAY

It is approved that this thesis has been written in compliance with the formatting rules laid down by the Graduate Institute of Sciences and Engineering.

Assist. Prof. Dr. Nurullah ARSLAN
Director

May 2007

Abdullah Said ERDOĞAN

M.S. Thesis In Mathematics

May 2007

NUMERICAL SOLUTIONS OF PARTIAL DIFFERENTIAL EQUATION WITH VARIABLE SPACE OPERATOR AND ITS APPLICATIONS

by

Abdullah Said ERDOĞAN

May 2007

NUMERICAL SOLUTIONS OF PARTIAL DIFFERENTIAL EQUATION WITH VARIABLE SPACE OPERATOR AND ITS APPLICATIONS

Abdullah Said ERDOĞAN

M. S. Thesis - Mathematics
May 2007

Supervisors: Prof. Dr. Allaberen ASHYRALYEV
Assist. Prof. Dr. Nurullah ARSLAN

ABSTRACT

In the present work computational blood flow analysis through glycocalyx on the endothelial cells is performed. Stable numerical schemes are developed for obtaining approximate solutions to the mixed problem for partial differential equation with variable space operator as the modeling blood flow through glycocalyx over endothelial cells. Numerical techniques are developed by applying a procedure of the solution of linear difference equation with matrix coefficients. The flow equations inside the core flow region and porous region are established. Discretization is done and the flow velocities in both regions are calculated. The wall shear stresses and the drag force over the glycocalyx is formulated. The effect of the flow over the glycocalyx is investigated.

Keywords: Parabolic equation, Difference schemes, Convergence, Stability, Blood flow, Endothelial cells, Glycocalyx, Wall shear stress.

DEĞİŞKEN UZAY OPERATÖRLÜ KISMİ DİFERANSİYEL DENKLEMLERİN NÜMERİK ÇÖZÜMLERİ VE UYGULAMALARI

Abdullah Said ERDOĞAN

Yüksek Lisans Tezi - Matematik
Mayıs 2007

Tez yöneticisi: Prof. Dr. Allaberen ASHYRALYEV
Yrd. Doç. Dr. Nurullah ARSLAN

ÖZ

Bu çalışmamızda endotel hücreler üzerinde bulunan glycocalyxlerin yüzeyi boyunca kan akış analizi yapılmıştır. Kararlı nümerik fark denklemleri oluşturularak endotel hücreler etrafındaki kan akışının matematiksel modellemesi olan değişken uzay operatörlü kısmi türevli diferansiyel denklem probleminin yaklaşık çözümü hesaplanmıştır.Matris katsayılı lineer fark denklemlerinin çözüm prosedürünün uygulandığı nümerik teknikler geliştirilmiştir. Düzgün akışın bulunduğu bölge ve poroz bölgede akış denklemleri oluşturulmuştur. Yüzey ağlara ayrılarak, her iki bölge için akış hızı hesaplanmıştır. Elde edilen bilgiler doğrultusunda çeper makaslama kuvveti ve sürtünme kuvveti hesaplanmıştır. Glycocalyxler üzerindeki akışın etkisi incelenmiştir.

Anahtar Kelimeler: Parabolik denklemler, Fark şemaları, Yakınsama, Kararlılık, Kan akışı, Endotel hücreler, Glycocalyx.

ACKNOWLEDGMENTS

I am glad to take this opportunity to thank firstly my supervisor Prof. Dr. Allaberen ASHYRALYEV and my co-supervisor Assist. Prof. Dr. Nurullah ARSLAN for their genuine help and very special encouragement throughout this research.

I would like to express my great appreciation to my collegues and friends for their valuable informations and comments on my academic and scientific problems.

TABLE OF CONTENTS

LIST OF FIGURES

FIGURE

LIST OF TABLES

TABLE

CHAPTER 1

INTRODUCTION

In mathematics, a partial differential equation is a relation involving an unknown function of several independent variables and its partial derivatives with respect to those variables. Partial differential equations are used to formulate and solve problems that involve unknown functions of several variables, such as the propagation of sound or heat, electrostatics, electrodynamics, fluid flow, elasticity, or more generally any process that is distributed in space, or distributed in space and time. Completely distinct physical problems may have identical mathematical formulations.

It is known that many applied problems in fluid mechanics, other areas of physics and mathematical biology were formulated as the mathematical model of partial differential equations of the variable types [Dehghan M.,2003] , [Cannon J.R., Perez Estava S. and van der Hoek J.,1987] , [Gordeziani N., Natani P. and Ricci P.E.,2005] , [Squire J.M., Chew M., Nneji G., Neal C., Barry J., Michel C.,2001] , [Ashyralyev A. and Ozdemir Y., 2005] and [Loth F.,Fischer P.F.,ArslanN., BertramC.D., LeeS.E., RoystonT.J., Shaalan W.E. and Bassiouny H.S.,2003] .

In this thesis, computational blood flow analysis through glycocalyx on the endothelial cells inside the arteries is performed by obtaining specific model of the blood flow over the EC. Endothelial surface glycocalyx was first detected by special electron microscopic staining techniques nearly forty years ago [Luft J.H.,1965], this surface layer has been observed lately in vivo [Vink H. and Duling B.R.,1996] and the importance of its multifaceted physiological functions recognized. Some of these functions are its role as a molecular sieve in determining the oncotic forces that are established across microvessel endothelium [Michel C.C.,1997],[Weinbaum S.,1998],[Hu X. and Weinbaum S.,1999] and [Hu X., Adamson R.H., Liu B., Curry F.E. and Weinbaum S.,2000] its role as a hydrodynamic exclusion layer preventing the interaction of proteins in the red cell and endothelial

cell membranes [Feng J. and Weinbaum S.,2000] , [Secomb T.W., Hsu R. and Pries A.R., 2001] and [Damiano E.R.,1998], its function in modulating leukocyte attachment and rolling [Zhao Y.H., Chien S. and Weinbaum S.,2001] and as a transducer of mechanical forces to the intracellular cytoskeleton in the initiation of intracellular signaling, as proposed herein. Fluid shearing forces acting on endothelial cells(EC) have a profound effect on EC morphology, structure, and function [Davies P.F.,1995]. It is now also clear from theoretical considerations [Feng J. and Weinbaum S.,2000], [Secomb T.W., Hsu R. and Pries A.R.,2001] , [Secomb T.W., Hsu R.and Pries A.R.,1998], [Damiano E.R.,1998] that the shear stress at the edge of the endothelial surface layer is greatly attenuated by the extracellular matrix of proteoglycans and glycoproteins in the glycocalyx with the result that fluid velocities, except near the edge of the layer, are vanishingly small. Thus, the shear stress due to the fluid flow acting on the apical membrane of the EC itself is negligible. This paradoxical prediction has raised a fundamental question as to how hydrodynamic and mechanical forces, more generally, are transmitted across the structural components of the glycocalyx. The computer-enhanced images showed that the glycocalyx is a 3D fibrous meshwork with a characteristic spacing of 20nm in all directions and that the effective diameter of the periodic scattering centers was 10–12 nm. A unique feature of the present analysis is the attempt to couple the dynamic response of the surface layer to mechanical loading to the stresses and deformations induced in the underlying cortical cytoskeleton.

It is known that the mixed problem for parabolic equations can be solved by Fourier series method, by Fourier transform method and by Laplace transform method. Now, let us illustrate these three different analytical methods by examples.

Example 1.1. First let us consider the simple boundary value problem for parabolic equation

$$\begin{cases} \frac{\partial u(t,x)}{\partial t} - \frac{\partial^2 u(t,x)}{\partial x^2} = -\frac{1}{4}e^{-\frac{t}{2}} \cos\frac{x}{2}, \ 0 < x < a, \ 0 < t < T, \\ \frac{\partial u(t,x)}{\partial t} - \frac{\partial^2 u(t,x)}{\partial x^2} + u(t,x) = \frac{3}{4}e^{-\frac{t}{2}} \cos\frac{x}{2}, \ a < x < \pi, \ 0 < t < T, \\ u_x(t,0) = u(t,\pi) = 0, \ u(t,a) = e^{-\frac{t}{2}} \cos\frac{a}{2}, \ u(0,x) = \cos\frac{x}{2}. \end{cases} \tag{1.1}$$

Solution. For the solution of the problem (1.1), we use the method of seperation of variables or so called Fourier Series Method. In order to solve the problem, first we need to introduce a new function :

$$z(t,x) = u(t,x) - e^{-\frac{t}{2}} \cos\frac{x}{2}.$$

So,

$$\begin{cases} \frac{\partial z(t,x)}{\partial t} - \frac{\partial^2 z(t,x)}{\partial x^2} = 0, \ 0 < x < a, \ 0 < t < T, \\ \frac{\partial z(t,x)}{\partial t} - \frac{\partial^2 z(t,x)}{\partial x^2} + z(t,x) = 0, \ a < x < \pi, \ 0 < t < T, \\ z_x(t,0) = z(t,\pi) = 0, \ z(t,a) = 0, \ z(0,x) = 0. \end{cases} \tag{1.2}$$

Now, let us obtain the solution of (1.2) by the method of separation of variables. To do this a solution of the form

$$z(t,x) = T(t)X(x) \neq 0$$

is suggested. Let $0 < x < a$ and take the partial derivatives and substituting the result in (1.2) , we obtain

$$\frac{T'(t)}{T(t)} - \frac{X''(x)}{X(x)} = 0,$$

or

$$\frac{T'(t)}{T(t)} = \frac{X''(x)}{X(x)} = \lambda.$$

Since

$$X''(x) = \lambda X(x), \; X'(0) = X(a) = 0,$$

we have that

$$X_k(x) = \cos\left(k + \frac{1}{2}\right)\frac{\pi}{a}, \; \lambda_k = -\left(k + \frac{1}{2}\right)^2, \; k = 0, 1, 2, \cdots.$$

Secondly for $a < x < \pi$,

$$\frac{T'(t)}{T(t)} = \frac{X''(x)}{X(x)} - 1 = \mu - 1, 0 < t < T.$$

Since

$$X''(x) = \mu X(x), \; X(a) = X(\pi) = 0,$$

we have the set of all non-trivial solutions

$$X_k(x) = \sin\left(\frac{k\pi}{\pi - a}\right) x \text{ and } X_k(x) = \cos\left(\frac{k\pi}{\pi - a}\right) \ x, a < x < \pi,$$
$$\mu_k = -\left(\frac{k\pi}{\pi - a}\right)^2, \ k = 0, 1, 2, \cdots.$$

So, we obtain the following results:

$$X_k(x) = \cos\left(k + \frac{1}{2}\right)\frac{\pi}{a}x \ , k = 0, 1, 2, \cdots, \ 0 < x < a,$$
$$X_k(x) = \sin\frac{k\pi}{\pi - a}x \text{ and } \cos\frac{k\pi}{\pi - a}x, k = 0, 1, 2, \cdots, \ a < x < \pi.$$

The solution for $T(t)$ can be obtained by using the Cauchy formula

$$T'(t) = -\left(k + \frac{1}{2}\right)^2 T(t) \Rightarrow T_k(t) = A_k e^{\left(k+\frac{1}{2}\right)^2 t}, \ 0 < x < a,$$

$$T'(t) = \left(-\left(\frac{k\pi}{\pi - a}\right)^2 - 1\right) T(t) \Rightarrow T_k(t) = B_k e^{\left(\left(\frac{k\pi}{\pi-a}\right)^2+1\right)t}, \ a < x < \pi.$$

By superposition principle

$$z(t,x) = \begin{cases} \sum\limits_{k=0}^{\infty} A_k e^{\left(k+\frac{1}{2}\right)^2 t} \cos\left(k + \frac{1}{2}\right)\frac{\pi}{a}x, 0 < x < a, \\ \sum\limits_{k=0}^{\infty} e^{\left(\left(\frac{k\pi}{\pi-a}\right)^2+1\right)t}\left(C_k \sin\frac{k\pi}{\pi-a}x + D_k \cos\frac{k\pi}{\pi-a}x\right), a < x < \pi. \end{cases}$$

Using the initial condition, we get

$$z(0,x) = \begin{cases} \sum\limits_{k=0}^{\infty} A_k \cos\left(k + \frac{1}{2}\right)\frac{\pi}{a}x, 0 < x < a, \\ \sum\limits_{k=0}^{\infty} C_k \sin\frac{k\pi}{\pi-a}x + D_k \cos\frac{k\pi}{\pi-a}x, a < x < \pi. \end{cases} = 0$$

$\Rightarrow A_k = 0$ and $C_k = D_k = 0$ (By taking $x = \pi - a$ and $x = \frac{\pi - a}{2}$ respectively.) Thus,

$$z(t,x) = 0$$

and

$$u(t,x) = e^{-\frac{t}{2}} \cos\frac{x}{2},\ 0 < x < \pi,\ 0 < t < 1.$$

Note that using the same manner one obtains the solution of the following boundary value problem for the multidimensional parabolic equation

$$\begin{cases} \frac{\partial u(t,x)}{\partial t} - \sum_{r=1}^{n} \alpha_r \frac{\partial^2 u(t,x)}{\partial x_r^2} = f(t,x), 0 < x_1 < a, \\ \\ \frac{\partial u(t,x)}{\partial t} - \sum_{r=1}^{n} \alpha_r \frac{\partial^2 u(t,x)}{\partial x_r^2} + \delta u(t,x) = g(t,x),\ a < x_1 < l_1, \\ \\ x = (x_1, \ldots, x_n) \in [0, l_1] \mathrm{x} \overline{\Omega}, 0 \le t \le T, \\ \\ u(t,x)|_{x_1 = a} = \psi(t), \frac{\partial u(t,0,x_2,\ldots x_n)}{\partial x_1} = 0, \\ u(t, l_1, x_2, ..x_n) = 0, u(0,x) = \varphi(x),\ x \in [0, l_1] \mathrm{x} \overline{\Omega}, \\ u(t,x) = 0, x \in [0, l_1] \mathrm{x} S, \end{cases}$$

where $\alpha_r > 0, \delta > 0$ and $f(t,x)$ $(t \in [0,T],\ x \in [0,a] \mathrm{x} \overline{\Omega})$, $g(t,x)$ $(t \in [0,T],\ x \in [a, l_1] \mathrm{x} \overline{\Omega})$, $\psi(t), \varphi(x)$ are given smooth functions. Here

$$\Omega = \{x = (x_2, .., x_k), 0 < x_k < l_k\}, 2 \le k \le n$$

with boundary

$$S, \ \ \overline{\Omega} = \Omega \cup S.$$

However, the method of separation of variables can be used only in the case when it has constant coefficients. It is well-known that the most useful method for solving partial differential equations with dependent coefficients in t and in the space variables is difference method.

Example 1.2. Another example for a parabolic equation is a mixed problem given below. It can be solved by Laplace transformation method (in t).

$$\begin{cases} \frac{\partial u}{\partial t} - \frac{\partial^2 u}{\partial x^2} = \frac{1}{4}\cos\frac{x}{2}, \ 0 < x < a, \ 0 < t < \infty, \\ \frac{\partial u}{\partial t} - \frac{\partial^2 u}{\partial x^2} + u = \frac{5}{4}\cos\frac{x}{2}, \ a < x < \pi, \ 0 < t < \infty, \\ u_x(t,0) = u(t,\pi) = 0, \ 0 < t < \infty, \\ u(0,x) = \cos\frac{x}{2}, \ 0 < x < \pi, \\ u(t,a+) = u(t,a-), \ u_x(t,a+) = u_x(t,a-), \ 0 < t < \infty. \end{cases}$$

Solution. Let $0 \leq x \leq a$. Then, taking the Laplace transform of both sides of the differential equation we can write that

$$\mathbf{L}\{u_t(t,x)\} - \mathbf{L}\{u_{xx}(t,x)\} = \mathbf{L}\left\{\frac{1}{4}\cos\frac{x}{2}\right\}$$

or

$$s\mathbf{L}\{u(t,x)\} - u(0,x) - (\mathbf{L}\{u(t,x)\})_{xx} = \frac{1}{4s}\cos\frac{x}{2}.$$

Let

$$\mathbf{L}\{u(t,x)\} = v(s,x).$$

So our problem becomes

$$sv\,(s,x) - v_{xx}\,(s,x) = \left(1 + \frac{1}{4s}\right)\cos\frac{x}{2}.$$

Now the complementary solution is

$$sv\,(s,x) - v_{xx}\,(s,x) = 0,$$

$$v_c\,(s,x) = C_1 e^{\sqrt{s}x} + C_2 e^{-\sqrt{s}x}$$

and the particular solution can be written as

$$v_p\,(s,x) = \ a\cos\frac{x}{2}.$$

Then

$$sa\cos\frac{x}{2} + \frac{a}{4}\cos\frac{x}{2} = \left(1 + \frac{1}{4s}\right)\cos\frac{x}{2}.$$

From that it follows $a = \frac{1}{s}$ and

$$v_p\,(s,x) = \frac{1}{s}\cos\frac{x}{2}.$$

So

$$v\,(s,x) = C_1 e^{\sqrt{s}x} + C_2 e^{-\sqrt{s}x} + \frac{1}{s}\cos\frac{x}{2}, 0 \le x \le a.$$

In the same manner, let take $a < x < \pi$.Then

$$\mathbf{L}\left\{u_t\left(t,x\right)\right\} - \mathbf{L}\left\{u_{xx}\left(t,x\right)\right\} + \mathbf{L}\left\{u\left(t,x\right)\right\} = \mathbf{L}\left\{\frac{5}{4}\cos\frac{x}{2}\right\}.$$

So our problem becomes

$$sv\left(s,x\right) - v_{xx}\left(s,x\right) + v\left(s,x\right) = \left(1+\frac{5}{4s}\right)\cos\frac{x}{2}.$$

Now the complementary solution is

$$\left(s+1\right)v\left(s,x\right) - v_{xx}\left(s,x\right) = 0,$$

$$v_c\left(s,x\right) = C_1 e^{\sqrt{s+1}x} + C_2 e^{-\sqrt{s+1}x}$$

and the particular solution can be written as

$$v_p\left(s,x\right) = \ a\cos\frac{x}{2}.$$

Then

$$\left(s+1\right)a\cos\frac{x}{2} + \frac{a}{4}\cos\frac{x}{2} = \left(1+\frac{5}{4s}\right)\cos\frac{x}{2}.$$

From that it follows $a = \frac{1}{s}$ and

$$v_p\left(s,x\right) = \frac{1}{s}\cos\frac{x}{2}.$$

So

$$v\left(s,x\right) = C_1 e^{\sqrt{s+1}x} + C_2 e^{-\sqrt{s+1}x} + \frac{1}{s}\cos\frac{x}{2},\ a < x < \pi.$$

By using the interface conditions at $x = a$, we can write

$$v(s,x) = \frac{1}{s}\cos\frac{x}{2}.$$

Hence taking the inverse of Laplace transform, we get

$$u(t,x) = \cos\frac{x}{2}, 0 \le x \le \pi.$$

Note that using the same manner one obtains the solution of the following boundary value problem for the multidimensional parabolic equation

$$\begin{cases} \frac{\partial u(t,x)}{\partial t} - \sum_{r=1}^{n} \alpha_r \frac{\partial^2 u(t,x)}{\partial x_r^2} = f(t,x), 0 < x_1 < a, \\ \\ \frac{\partial u(t,x)}{\partial t} - \sum_{r=1}^{n} \alpha_r \frac{\partial^2 u(t,x)}{\partial x_r^2} + \delta u(t,x) = g(t,x),\ a < x_1 < l_1, \\ \\ x = (x_1, \ldots, x_n) \in [0,l_1]\,\mathrm{x}\overline{\Omega}, 0 \le t < \infty, \\ \\ \frac{\partial u(t,0,x_2,\ldots x_n)}{\partial x_1} = 0, u(t,l_1,x_2,..x_n) = 0, \\ u(t,x)|_{x_1=a+} = u(t,x)|_{x_1=a-}\ , \left.\frac{\partial u(t,x)}{\partial x_1}\right|_{x_1=a+} = \left.\frac{\partial u(t,x)}{\partial x_1}\right|_{x_1=a-}, \\ u(0,x) = \varphi(x),\ x \in [0,l_1]\,\mathrm{x}\overline{\Omega}, \\ \\ u(t,x) = 0, x \in [0,l_1]\,\mathrm{x}S, \end{cases}$$

where $\alpha_r > 0, \delta > 0$ and $f(t,x)$ $(t \in [0,\infty),\ x \in [0,a]\mathrm{x}\overline{\Omega})$, $g(t,x)$ $(t \in [0,\infty),\ x \in [a,l_1]\mathrm{x}\overline{\Omega})$, $\varphi(x)$ are given smooth functions. Here

$$\Omega = \{x = (x_2,..,x_k), 0 < x_k < l_k\}, 2 \le k \le n$$

with boundary

$$S, \ \ \overline{\Omega} = \Omega \cup S.$$

However, Laplace transform method can be used only in the case when it has constant coefficients. It is well-known that the most useful method for solving partial differential equations with dependent coefficients in t and in the space variables is difference method.

Example 1.3. The last example is a mixed problem solved by using Fourier Transform method.

$$\frac{\partial u}{\partial t} - \frac{\partial^2 u}{\partial x^2} = \left(\frac{1}{4} - 2t\right) e^{-t^2} \cos\frac{x}{2}, \ 0 < x < a, \ \ -\infty < t < \infty,$$

$$\frac{\partial u}{\partial t} - \frac{\partial^2 u}{\partial x^2} + u = \left(\frac{5}{4} - 2t\right) e^{-t^2} \cos\frac{x}{2}, \ a < x < \pi, \ \ -\infty < t < \infty,$$

$$u_x(t, 0) = u(t, \pi) = 0, \ \ -\infty < t < \infty,$$

$$u\left(t,a+\right)=u\left(t,a-\right),\ u_x\left(t,a+\right)=u_x\left(t,a-\right),-\infty<t<\infty.$$

Solution. Let $0<x<a$. By taking the Fourier transform of both sides, we obtain

$$\mathbf{F}\{u_t\left(t,x\right)\}-\mathbf{F}\{u_{xx}\left(t,x\right)\}=\mathbf{F}\left\{\left(\frac{1}{4}-2t\right)e^{-t^2}\cos\frac{x}{2}\right\},$$

$$u_x\left(s,0\right)=u\left(s,\pi\right)=0.$$

Denote that

$$F\left\{u\left(t,x\right)\right\}=v\left(s,x\right).$$

Then we have

$$isv\left(s,x\right)-v_{xx}\left(s,x\right)=\cos\frac{x}{2}F\left\{\frac{1}{4}e^{-t^2}-2te^{-t^2}\right\}$$

or

$$isv\left(s,x\right)-v_{xx}\left(s,x\right)=\cos\frac{x}{2}\left(F\left\{\frac{1}{4}e^{-t^2}\right\}+F\left\{-2te^{-t^2}\right\}\right)$$
$$isv\left(s,x\right)-v_{xx}\left(s,x\right)=\cos\frac{x}{2}\left(\frac{1}{4}F\left\{e^{-t^2}\right\}+isF\left\{e^{-t^2}\right\}\right).$$

The complementary solution is

$$isv\left(s,x\right)-v_{xx}\left(s,x\right)=0,$$

$$v_c\left(s,x\right)=C_1e^{\sqrt{is}x}+C_2e^{-\sqrt{is}x}$$

and the particular solution can be written as

$$v_p\left(s,x\right)=\ a\cos\frac{x}{2}.$$

Then

$$isa\cos\frac{x}{2}+\frac{a}{4}\cos\frac{x}{2}=\left(\frac{1}{4}F\left\{e^{-t^2}\right\}+isF\left\{e^{-t^2}\right\}\right)\cos\frac{x}{2}.$$

It follows that $a=F\left\{e^{-t^2}\right\}$ and

$$v_p\left(s,x\right)=F\left\{e^{-t^2}\right\}\cos\frac{x}{2}.$$

So

$$v\left(s,x\right)=C_1e^{\sqrt{is}x}+C_2e^{-\sqrt{is}x}+F\left\{e^{-t^2}\right\}\cos\frac{x}{2},0<x<a.$$

Let $a<x<\pi$. In the same manner

$$\mathbf{F}\{u_t\left(t,x\right)\}-\mathbf{F}\{u_{xx}\left(t,x\right)\}+F\left\{u\left(t,x\right)\right\}=\mathbf{F}\left\{\left(\frac{5}{4}-2t\right)e^{-t^2}\cos\frac{x}{2}\right\}.$$

Then we have

$$isv\left(s,x\right)-v_{xx}\left(s,x\right)+v\left(s,x\right)=\cos\frac{x}{2}F\left\{\frac{5}{4}e^{-t^{2}}-2te^{-t^{2}}\right\}$$

or

$$\left(is+1\right)v\left(s,x\right)-v_{xx}\left(s,x\right)=\cos\frac{x}{2}\left(F\left\{\frac{5}{4}e^{-t^{2}}\right\}+F\left\{-2te^{-t^{2}}\right\}\right)$$
$$\left(is+1\right)v\left(s,x\right)-v_{xx}\left(s,x\right)=\cos\frac{x}{2}\left(\frac{5}{4}F\left\{e^{-t^{2}}\right\}+isF\left\{e^{-t^{2}}\right\}\right).$$

The complementary solution is

$$\left(is+1\right)v\left(s,x\right)-v_{xx}\left(s,x\right)=0,$$

$$v_{c}\left(s,x\right)=C_{1}e^{\sqrt{is+1}x}+C_{2}e^{-\sqrt{is+1}x}$$

and the particular solution can be written as

$$v_{p}\left(s,x\right)=\ a\cos\frac{x}{2}.$$

Then

$$\left(is+1\right)a\cos\frac{x}{2}+\frac{a}{4}\cos\frac{x}{2}=\left(\frac{5}{4}F\left\{e^{-t^{2}}\right\}+isF\left\{e^{-t^{2}}\right\}\right)\cos\frac{x}{2}.$$

It follows that $a=F\left\{e^{-t^{2}}\right\}$ and

$$v_{p}\left(s,x\right)=F\left\{e^{-t^{2}}\right\}\cos\frac{x}{2}.$$

So

$$v(s,x) = C_1 e^{\sqrt{is+1}x} + C_2 e^{-\sqrt{is+1}x} + F\left\{e^{-t^2}\right\}\cos\frac{x}{2},\ a < x < \pi.$$

By using the interface conditions at $x = a$, we can write

$$v(s,x) = F\left\{e^{-t^2}\right\}\cos\frac{x}{2}\ , 0 < x < \pi.$$

Hence taking the inverse of Fourier transform, we get

$$u(t,x) = e^{-t^2}\cos\frac{x}{2}, 0 \le x \le \pi.$$

Note that using the same manner one obtains the solution of the following boundary value problem for the multidimensional parabolic equation

$$\begin{cases} \frac{\partial u(t,x)}{\partial t} - \sum\limits_{r=1}^{n} \alpha_r \frac{\partial^2 u(t,x)}{\partial x_r^2} = f(t,x), 0 < x_1 < a, \\ \\ \frac{\partial u(t,x)}{\partial t} - \sum\limits_{r=1}^{n} \alpha_r \frac{\partial^2 u(t,x)}{\partial x_r^2} + \delta u(t,x) = g(t,x),\ a < x_1 < l_1, \\ \\ x = (x_1, \ldots, x_n) \in [0, l_1]\, \mathrm{x}\overline{\Omega}, -\infty < t < \infty, \\ \\ \frac{\partial u(t,0,x_2,\ldots x_n)}{\partial x_1} = 0, u(t, l_1, x_2, ..x_n) = 0, \\ u(t,x)|_{x_1=a+} = u(t,x)|_{x_1=a-}\ , \left.\frac{\partial u(t,x)}{\partial x_1}\right|_{x_1=a+} = \left.\frac{\partial u(t,x)}{\partial x_1}\right|_{x_1=a-}, \\ \\ u(t,x) = 0, x \in [0, l_1]\, \mathrm{x}S, \end{cases}$$

where $\alpha_r > 0, \delta > 0$ and $f(t,x)$ $(t \in (-\infty, \infty)\,,\ x \in [0,a]\mathrm{x}\overline{\Omega})$, $g(t,x)$ $(t \in (-\infty, \infty)\,,\ x \in$

$[a, l_1]\mathrm{x}\overline{\Omega})$, $\varphi(x)$ are given smooth functions. Here

$$\Omega = \{x = (x_2, .., x_k), 0 < x_k < l_k\}, 2 \leq k \leq n$$

with boundary

$$S, \ \overline{\Omega} = \Omega \cup S.$$

However, the Fourier transform method can be used only in the case when it has constant coefficients. It is well-known that the most useful method for solving partial differential equations with dependent coefficients in x and in the space variables is difference method.

In the present work the difference schemes of the first and second order of accuracy for the numerical solution of the mixed problem for one dimensional diffusion equation with variable space operator

$$\begin{cases} \frac{\partial u(t,x)}{\partial t} = \frac{\partial}{\partial x}(a(t,x)\frac{\partial u(t,x)}{\partial x}) + f(t,x), x \in (0,l), t \in [0,T], \\ \frac{\partial u(t,x)}{\partial t} = \frac{\partial}{\partial x}(a(t,x)\frac{\partial u(t,x)}{\partial x}) + b(t,x)u(t,x) + g(t,x), x \in (l,L), t \in [0,T], \\ u(0,x) = \varphi(x), x \in [0,L], \\ u_x(t,0) = 0, u(t,L) = 0, t \in [0,T], \\ u(t,l+) = u(t,l-), u_x(t,l+) = u_x(t,l-), t \in [0,T], \end{cases} \tag{1.3}$$

are considered. Applying the operator approach the stability estimates for solution of these difference schemes are obtained. The theoretical statements for the solution of this difference schemes are supported by the results of numerical experiments. In applications,

the cause of atherosclerosis which is the leading reason of illness and death is investigated. The blood flow equations inside the core flow region and porous region are calculated and the wall shear stresses and the drag force over the glycocalyx are formulated.

Let us briefly describe the contents of the various sections. It consists of seven chapters.

First chapter is the introduction.

Second chapter presents elementary statements in a Hilbert space that is needed for this work.

Third chapter presents first and second order of difference schemes and their numerical analysis.

Fourth chapter presents r-modified Crank-Nicholson difference scheme and its numerical analysis.

Fifth chapter is the application in the field of biomechanics. The description of the problem and the solving methods are presented. Constructed difference schemes are performed for the problem. The figures and table are included. Results of the application is given in this chapter.

Sixth chapter is the conclusion.

Seventh chapter is the algorithm and programming for the given applications.

1.1. Starting Point

Our starting point in this thesis is a representation ,given by Karin Leidermann from University of UTAH, named as A Closer Look at the Capillary Endothelial Glycocalyx.The representation starts with an investigation on the Navier Stokes equations in cylindrical coordinates

$$U = U(R, Z, \theta),$$

assuming fully developed, unidirectional flow in rigid tube such as

$$\frac{\partial U}{\partial t} = \frac{\partial U}{\partial Z} = \frac{\partial U}{\partial \theta} = 0.$$

And

$$\frac{\partial P}{\partial Z} = \mu \frac{1}{R} \frac{\partial}{\partial R}(R \frac{\partial U_c}{\partial R}),$$

$$\frac{\partial P}{\partial Z} = \mu \frac{1}{R} \frac{\partial}{\partial R}(R \frac{\partial U_c}{\partial R}) - F_z, \tag{1.4}$$

where

$$F_z = \frac{\mu U_g}{K_p}.$$

Here (1.4) also known as the Brinkman equation and K_p is Darcy permeabiality, describes how densely the proteoglycans are packed.

To simplify a bit, we can non-dimensionalize the equations using these changes of variables:

$$U = U'u, R = R'r, Z = R'z, P = P'p = \frac{\mu U'}{R'},$$

where U', R' and P' are the characteristic velocity, length and pressure. So,

$$\frac{\partial P}{\partial Z} = \frac{1}{r}\frac{\partial}{\partial r}(r\frac{\partial U_c}{\partial r}),$$

$$\frac{\partial P}{\partial Z} = \frac{1}{r}\frac{\partial}{\partial r}(r\frac{\partial U_g}{\partial r}) - \alpha^2 u_g,$$

where

$$\alpha^2 = \frac{R'}{\sqrt{K_p}}.$$

For constructing the boundary and matching conditions, in the representation the velocities and shear stress to match at the edge of the glycocalyx and no-slip condition at the endothelial cell membrane, $(r = 1)$ at the symmetry in the center are given as follows

$$\begin{aligned} u_c(r_g) &= u_g(r_g), \\ \frac{\tau\partial u_c(r_g)}{\partial r} &= \frac{\tau\partial u_g(r_g)}{\partial r}, \\ u_g(1) = 0,\ &\frac{\partial u_c(0)}{\partial r} = 0. \end{aligned}$$

For solving core flow velocity u_c, an assumption was done as

$$\frac{\partial}{\partial z}\frac{\partial p}{\partial z} = \frac{\partial}{\partial z}(\frac{1}{r}\frac{\partial}{\partial r}(r\frac{\partial U_c}{\partial r})) \Rightarrow \frac{\partial^2 p}{\partial z^2} = 0 \Rightarrow \frac{\partial p}{\partial z} = constant,$$

where the pressure gradient is constant throughout the tube. Integrating up twice and using a matching condition and a boundary condition.Finally

$$u_c = -\frac{1}{4}\frac{\partial p}{\partial z}(r_g^2 - r^2) + u_g(r_g)$$

was obtained.

And for solving the velocity u_g inside porous media, the Brinkman equation was rewritten in the form:

$$r^2(u_g)_{rr} + r(u_g)_r - r^2\alpha^2 u_g = \frac{\partial p}{\partial z}r^2,$$

which looks like an inhomogeneous Bessel equation where normal Bessel equation takes the form

$$x^2y'' + xy' + (\lambda x^2 - r^2)y = 0.$$

By using the solution of the Bessel functions, a particular solution

$$(u_g)_p = -\frac{1}{\alpha^2}\frac{\partial p}{\partial z}$$

was obtained.

Still solving for u_g , some more approximations and calculation of coefficients can be done as

$$\tilde{A} = \frac{\frac{-\partial p}{\alpha^2 \partial z}(\frac{\alpha r_g}{2} - \frac{K_1(\alpha r_g)}{K_0(\alpha)})}{\frac{K_1(\alpha r_g)}{K_0(\alpha)} + \frac{I_1(\alpha r_g)}{I_0(\alpha)}} \approx \frac{-\partial p}{\alpha^2 \partial z}(-1) = \frac{-\partial p}{\alpha^2 \partial z}C_1,$$
$$\tilde{B} = \frac{\frac{-\partial p}{\alpha^2 \partial z}(\frac{\alpha r_g}{2} - \frac{I_1(\alpha r_g)}{I_0(\alpha)})}{\frac{K_1(\alpha r_g)}{K_0(\alpha)} + \frac{I_1(\alpha r_g)}{I_0(\alpha)}} \approx \frac{-\partial p}{\alpha^2 \partial z}(\frac{\frac{\alpha r_g}{2}}{\frac{K_1(\alpha r_g)}{K_0(\alpha)}}) = \frac{-\partial p}{\alpha^2 \partial z}C_2,$$
$$u_c(r) = -\frac{1}{4}\frac{\partial p}{\partial z}(r_g^2 - r^2) + u_g(r_g) = -\frac{1}{4}\frac{\partial p}{\partial z}(r_g^2 - r^2) + \frac{-\partial p}{\alpha^2 \partial z}C_3.$$

After using the boundary conditions, matching conditions, the final solutions are given by

$$u_c(r) = -\frac{1}{4}\frac{\partial p}{\partial z}(r_g^2 - r^2) + \frac{-\partial p}{\alpha^2 \partial z}(\frac{r_g \alpha}{2} + 1)$$
$$u_g(r) = -\frac{\partial p}{\alpha^2 \partial z}(-\frac{I_0(r\alpha)}{I_o(\alpha)} + \frac{r_g \alpha}{2}\frac{K_0(r\alpha)}{K_1(r_g\alpha)} + 1)$$

In the next step calculation of drag force was given. Darcy permeability and the

volume fraction of the proteoglycans are given by:

$$K_p = \frac{\ln(c^{-1/2}) - 0.745 + c - \frac{c^2}{4} + O(c^4)}{4\pi}, c = \frac{\pi a_p^2}{(2a_p + \Delta)^2 \frac{\sqrt{3}}{2}},$$

where

$$\Delta = 50nm \text{ (proteoglycans are approximately 50 nm apart)},$$
$$a_p = 5nm \text{ (protein radius)},$$
$$U' = 0.1cms^{-1}$$

and

$$K_p = 278.03nm^2 \text{ and } c = 0.0252.$$

So,

$$F_{drag} = \frac{\pi \mu U_g(R) a_p^2}{cK_p} \approx 1.36 \text{ x } 10^{-2} u_g \frac{pN}{nm}.$$

CHAPTER 2

HILBERT SPACES METHODS

2.1. Hilbert Space

Definition. A complex linear space H is called an inner product space if there is a complex-valued function $\langle .,. \rangle : H \times H \to C$ with the properties

$$
\begin{aligned}
&i. \quad \langle x,x \rangle \geq 0 \text{ and } \quad \langle x,x \rangle = 0 \Longleftrightarrow \quad x = \widetilde{0}, \\
&ii. \ \langle x,y \rangle = \overline{\langle y,x \rangle} \quad \forall x,y \in H \ , \\
&iii. \langle \alpha x,y \rangle = \alpha \langle x,y \rangle , \qquad \forall x,y \in H \quad \text{and } \alpha \in C, \\
&iv. \langle x+y,z \rangle = \langle x,z \rangle + \langle y,z \rangle \quad \forall \ x,y,z \in H.
\end{aligned}
$$

The function $\langle x,y \rangle$ is called the inner product of x and y, C is the set of complex numbers and the over-line indicates the complex conjugate. A Hilbert space is a complete inner product space. An inner product on H defines a norm on H given by $\|x\| = \langle x,x \rangle^{1/2}$.

2.2. Bounded Linear Operators in H

Definition. Let H_1 and H_2 are two Hilbert spaces. An operator $A : H_1 \to H_2$ is said to be linear operator if

$$A(\alpha x + \beta y) = \alpha Ax + \beta Ay \quad \text{for all} \quad \alpha, \beta \in C \ \text{ and } x, y \in H_1.$$

$D(A) = \{x \in H_1, \exists Ax \in H_2\}$ is the domain of A and is a vector space and

$R(A) = \{y = Ax, \forall x \in D(A)\}$ denotes the range of A.

A linear operator $A : H \to H$ is said to be bounded if there exist a real number $M > 0$ such that

$$\|Ax\|_H \leq M \ \|x\|_H \qquad for\ all\ \ x \in H.$$

If a linear operator $A : H \to H$ is bounded with M, then

$$\|A\| = \inf M$$

is called the norm of operator A.

Theorem 2.2.1. The norm of the bounded linear operator A is

$$\|A\| = \sup_{\|x\| \leq 1} \|Ax\| \ = \sup_{x \neq \tilde{0}} \frac{\|Ax\|}{\|x\|} \ = \ \sup_{\|x\|=1} \|Ax\| .$$

An example can be given as A is an operator defined by $Ax = \alpha x(t)$,

$A : L_2[0,1] \longrightarrow L_2[0,1]$ .Then, $\|A\| = |\alpha|$.

2.3. Adjoint of an Operator

Definition. Let $A : H_1 \to H_2$ be a bounded linear operator, where H_1 and H_2 are Hilbert spaces. Then the Hilbert adjoint operator A^* of A is the operator

$$A^* : H_2 \to H_1,$$

such that for all $x \in H_1$ and $y \in H_2$

$$\langle Ax, y\rangle = \langle x, A^* y\rangle .$$

Theorem 2.3.1. The Hilbert adjoint operator A^* of A is unique and bounded linear operator with the norm

$$\|A^*\| = \|A\| .$$

Definition. A bounded linear operator $A : H \longrightarrow H$ on a Hilbert space H is said to be self-adjoint if $\langle Ax, y\rangle = \langle x, Ay\rangle$ for all $x, y \in H$.

Definition. A self-adjoint operator A is said to be positive if $A \geq 0$, that is $(Ax, x) \geq 0$ for all $x \in H$.

Example 2.3.1. Consider the operator

$$Au = \begin{cases} -\frac{d}{dx}\left(a\left(x\right)\frac{du(x)}{dx}\right) \ , \ 0 \leq x < l \\ -\frac{d}{dx}\left(a\left(x\right)\frac{du(x)}{dx}\right) + au\left(x\right) \ , \ l < x \leq L \end{cases}$$

with domain

$$D\left(A\right) = \{u, u', u'' \in L_2\left[0, L\right] \text{ and } u\left(l-\right) = u\left(l+\right) \ , \ u_x\left(l-\right) = u_x\left(l+\right) \ , \ u_x\left(0\right) = u\left(L\right) = 0\} .$$

Here $a\left(x\right)$ is sufficiently smooth function and $a\left(x\right) \geq a > 0$. A is the positive, self-adjoint operator.

Solution. Using the additivity property of definite integral and applying the formula of integration by parts , we obtain

$$\langle u, Av\rangle = \int_0^L u(r)\, Av(r)\, dr = \int_0^l u(r)\, Av(r)\, dr + \int_l^L u(r)\, Av(r)\, dr$$

$$= -\int_0^l u(r)\left[a(r)\, v'(r)\right]' dr - \int_l^L u(r)\left[a(r)\, v'(r)\right]' dr + a\int_l^L u(r)\, v(r)\, dr$$

$$= -u(r)\, a(r)\, v'(r)\Big]_0^l + \int_0^l u'(r)\, a(r)\, v'(r)\, dr - u(r)\, a(r)\, v'(r)\Big]_l^L$$

$$+ \int_l^L u'(r)\, a(r)\, v'(r)\, dr + a\int_l^L u(r)\, v(r)\, dr$$

$$= -u(l)\, a(l)\, v'(l) + u(0)\, a(0)\, v'(0) - u(L)\, a(L)\, v'(L) + u(l)\, a(l)\, v'(l)$$

$$+ \int_0^l u'(r)\, a(r)\, v'(r)\, dr + \int_l^L u'(r)\, a(r)\, v'(r)\, dr + a\int_l^L u(r)\, v(r)\, dr$$

$$= \int_0^l u'(r)\, a(r)\, v'(r)\, dr + \int_l^L u'(r)\, a(r)\, v'(r)\, dr + a\int_l^L u(r)\, v(r)\, dr,$$

$$\langle Au, v\rangle = \int_0^l Au\,(r)\,v\,(r)\,dr + \int_l^L Au\,(r)\,v\,(r)\,dr = \int_0^L Au\,(r)\,v\,(r)\,dr$$

$$= -\int_0^l [a\,(r)\,u'\,(r)]'\,v\,(r)\,dr - \int_l^L [a\,(r)\,u'\,(r)]'\,v\,(r)\,dr + a\int_l^L u\,(r)\,v\,(r)\,dr$$

$$-u'\,(r)\,a\,(r)\,v\,(r)]_0^l + \int_0^l u'\,(r)\,a\,(r)\,v'\,(r)\,dr\; -u'\,(r)\,a\,(r)\,v\,(r)]_l^L$$

$$= \int_l^L u'\,(r)\,a\,(r)\,v'\,(r)\,dr + a\int_l^L u\,(r)\,v\,(r)\,dr$$

$$-u'\,(l)\,a\,(l)\,v\,(l) + u'\,(0)\,a\,(0)\,v\,(0) - u'\,(L)\,a\,(L)\,v\,(L) + u'\,(l)\,a\,(l)\,v\,(l)$$

$$= \int_0^l u'\,(r)\,a\,(r)\,v'\,(r)\,dr + \int_l^L u'\,(r)\,a\,(r)\,v'\,(r)\,dr + a\int_l^L u\,(r)\,v\,(r)\,dr. \tag{2.1}$$

Then $\langle u, Av\rangle = \langle Au, v\rangle$. This means that $A = A^*$. Moreover, using equality (2.1), we obtain that

$$\begin{aligned}\langle Au, u\rangle &= \int_0^l u'(r)\, a(r)\, u'(r)\, dr + \int_l^L u'(r)\, a(r)\, u'(r)\, dr + a\int_l^L u(r)\, u(r)\, dr \\ &= \int_0^l a(r)\,(u'(r))^2\, dr + \int_l^L a(r)\,(u'(r))^2\, dr + a\int_l^L (u(r))^2\, dr\end{aligned}$$

$$\begin{aligned}&\geq a\int_0^l (u'(r))^2\, dr + a\int_l^L (u'(r))^2\, dr + a\int_l^L (u(r))^2\, dr \\ &= a\int_0^L (u'(r))^2\, dr + a\int_l^L (u(r))^2\, dr \geq 0.\end{aligned}$$

So A is the positive operator.

Example 2.3.2. Consider the difference operator

$$A_h u^h = \begin{pmatrix} -\frac{u^{n+1}-2u^n+u^{n-1}}{h^2},\ 1 \leq n \leq M_l - 1 \\ -\frac{u^{n+1}-2u^n+u^{n-1}}{h^2} + u^n,\ M_l + 1 \leq n \leq M - 1 \end{pmatrix}$$

with

$$u^0 = u^1\ ,\ u^M = 0\ ,\ u^{M_l+1} - u^{M_l} = u^{M_l} - u^{M_l-1}.$$

Here

$$u^h = \{u^n\}_0^M$$

and

$$Mh = L \ .$$

Solution. Applying Abel's formula, we can write

$$\left\langle A_h u^h, v^h \right\rangle = \sum_{n=1}^{M_l-1} \left(A_h u^h\right)^n \left(v^h\right)^n h + \sum_{n=M_l+1}^{M-1} \left(A_h u^h\right)^n \left(v^h\right)^n h$$

$$= \sum_{n=1}^{M_l-1} \left(-\frac{u^{n+1} - 2u^n + u^{n-1}}{h^2} \right) v^n h + \sum_{n=M_l+1}^{M-1} \left(-\frac{u^{n+1} - 2u^n + u^{n-1}}{h^2} + u^n \right) v^n h$$

$$= -\sum_{n=1}^{M_l-1} \left(\frac{\frac{u^{n+1}-u^n}{h} - \frac{u^n-u^{n-1}}{h}}{h} \right) v^n h - \sum_{n=M_l+1}^{M-1} \left(\frac{\frac{u^{n+1}-u^n}{h} - \frac{u^n-u^{n-1}}{h}}{h} \right) v^n h + \sum_{n=M_l+1}^{M-1} u^n v^n h$$

$$= -\frac{1}{h} \left(\sum_{n=1}^{M_l-1} \left(u^{n+1} - u^n\right) v^n - \left(u^n - u^{n-1}\right) v^n \right)$$
$$- \frac{1}{h} \left(\sum_{n=M_l+1}^{M-1} \left(u^{n+1} - u^n\right) v^n - \left(u^n - u^{n-1}\right) v^n \right) + \sum_{n=M_l+1}^{M-1} u^n v^n h$$

$$= -\frac{1}{h} \left(\sum_{n=1}^{M_l-1} \left(u^{n+1} - u^n\right) v^n - \sum_{n=1}^{M_l-1} \left(u^n - u^{n-1}\right) v^n \right)$$
$$- \frac{1}{h} \left(\sum_{n=M_l+1}^{M-1} \left(u^{n+1} - u^n\right) v^n - \sum_{n=M_l+1}^{M-1} \left(u^n - u^{n-1}\right) v^n \right) + \sum_{n=M_l+1}^{M-1} u^n v^n h$$

$$= -\frac{1}{h}\left(\sum_{n=2}^{M_l}\left(u^n - u^{n-1}\right)v^{n-1} - \sum_{n=1}^{M_l-1}\left(u^n - u^{n-1}\right)v^n\right)$$
$$-\frac{1}{h}\left(\sum_{n=M_l+2}^{M}\left(u^n - u^{n-1}\right)v^{n-1} - \sum_{n=M_l+1}^{M-1}\left(u^n - u^{n-1}\right)v^n\right) + \sum_{n=M_l+1}^{M-1} u^n v^n h$$

$$= \frac{1}{h}\sum_{n=2}^{M_l-1}\left(u^n - u^{n-1}\right)\left(v^n - v^{n-1}\right) + \frac{1}{h}\sum_{n=M_l+2}^{M-1}\left(u^n - u^{n-1}\right)\left(v^n - v^{n-1}\right)$$
$$+ \sum_{n=M_l+1}^{M-1} u^n v^n h - \left(u^{M_l} - u^{M_l-1}\right)v^{M_l-1} + \left(u^1 - u^0\right)v^1$$
$$- \left(u^M - u^{M-1}\right)v^{M-1} + \left(u^{M_l+1} - u^{M_l}\right)v^{M_l+1}$$

$$= \frac{1}{h}\sum_{n=2}^{M_l-1}\left(u^n - u^{n-1}\right)\left(v^n - v^{n-1}\right) + \frac{1}{h}\sum_{n=M_l+2}^{M-1}\left(u^n - u^{n-1}\right)\left(v^n - v^{n-1}\right)$$
$$+ \sum_{n=M_l+1}^{M-1} u^n v^n h - \left(u^{M_l} - u^{M_l-1}\right)\left(v^{M_l-1} - v^{M_l}\right) + u^{M-1}v^{M-1}$$
$$+ \left(u^{M_l+1} - u^{M_l}\right)\left(v^{M_l+1} - v^{M_l}\right) + v^{M_l}\left(\left(u^{M_l+1} - u^{M_l}\right) - \left(u^{M_l} - u^{M_l-1}\right)\right)$$

$$= \frac{1}{h}\sum_{n=2}^{M_l-1}\left(u^n - u^{n-1}\right)\left(v^n - v^{n-1}\right) + \frac{1}{h}\sum_{n=M_l+2}^{M-1}\left(u^n - u^{n-1}\right)\left(v^n - v^{n-1}\right) \tag{2.2}$$
$$+ \sum_{n=M_l+1}^{M-1} u^n v^n h + \left(u^{M_l} - u^{M_l-1}\right)\left(v^{M_l-1} - v^{M_l}\right) + u^{M-1}v^{M-1}$$
$$+ \left(u^{M_l+1} - u^{M_l}\right)\left(v^{M_l+1} - v^{M_l}\right),$$

$$\left\langle u^h, A_h v^h\right\rangle = \sum_{n=1}^{M_l-1}\left(u^h\right)^n\left(A_h v^h\right)^n h + \sum_{n=M_l+1}^{M-1}\left(u^h\right)^n\left(A_h v^h\right)^n h$$

$$= \sum_{n=1}^{M_l-1} u^n \left(-\frac{v^{n+1} - 2v^n + v^{n-1}}{h^2} \right) h + \sum_{n=M_l+1}^{M-1} u^n \left(-\frac{v^{n+1} - 2v^n + v^{n-1}}{h^2} + v^n \right) h$$

$$= -\sum_{n=1}^{M_l-1} u^n \left(\frac{\frac{v^{n+1}-v^n}{h} - \frac{v^n - v^{n-1}}{h}}{h} \right) h - \sum_{n=M_l+1}^{M-1} u^n \left(\frac{\frac{v^{n+1}-v^n}{h} - \frac{v^n - v^{n-1}}{h}}{h} \right) h + \sum_{n=M_l+1}^{M-1} u^n v^n h$$

$$\begin{aligned}
&= -\frac{1}{h} \left(\sum_{n=1}^{M_l-1} u^n \left(v^{n+1} - v^n \right) - u^n \left(v^n - v^{n-1} \right) \right) \\
&- \frac{1}{h} \left(\sum_{n=M_l+1}^{M-1} u^n \left(v^{n+1} - v^n \right) - u^n \left(v^n - v^{n-1} \right) \right) + \sum_{n=M_l+1}^{M-1} u^n v^n h \\
&= -\frac{1}{h} \left(\sum_{n=1}^{M_l-1} u^n \left(v^{n+1} - v^n \right) - \sum_{n=1}^{M_l-1} u^n \left(v^n - v^{n-1} \right) \right) \\
&- \frac{1}{h} \left(\sum_{n=M_l+1}^{M-1} u^n \left(v^{n+1} - v^n \right) - \sum_{n=M_l+1}^{M-1} u^n \left(v^n - v^{n-1} \right) \right) + \sum_{n=M_l+1}^{M-1} u^n v^n h
\end{aligned}$$

$$\begin{aligned}
&= \frac{1}{h} \sum_{n=2}^{M_l-1} u^n \left(v^n - v^{n-1} \right) - \frac{1}{h} \sum_{n=2}^{M_l-1} u^{n-1} \left(v^n - v^{n-1} \right) \\
&+ \frac{1}{h} \sum_{n=M_l+2}^{M-1} u^n \left(v^n - v^{n-1} \right) - \frac{1}{h} \sum_{n=M_l+2}^{M-1} u^{n-1} \left(v^n - v^{n-1} \right) \\
&+ \sum_{n=M_l+1}^{M-1} u^n v^n h - u^{M_l} \left(v^{M_l+1} - v^{M_l-1} \right) + u^1 \left(v^1 - v^0 \right) \\
&- u^{M-1} \left(v^M - v^{M-1} \right) + u^{M_l+1} \left(v^{M_l+1} - v^{M_l-1} \right).
\end{aligned}$$

$$= \frac{1}{h}\sum_{n=2}^{M_l-1}\left(u^n-u^{n-1}\right)\left(v^n-v^{n-1}\right)+\frac{1}{h}\sum_{n=M_l+2}^{M-1}\left(u^n-u^{n-1}\right)\left(v^n-v^{n-1}\right)$$
$$+\sum_{n=M_l+1}^{M-1}u^nv^nh-\left(u^{M_l}-u^{M_l-1}\right)\left(v^{M_l-1}-v^{M_l}\right)+u^{M-1}v^{M-1}$$
$$+\left(u^{M_l+1}-u^{M_l}\right)\left(v^{M_l+1}-v^{M_l}\right)+u^{M_l}\left(\left(v^{M_l+1}-v^{M_l}\right)-\left(v^{M_l}-v^{M_l-1}\right)\right)$$

$$= \frac{1}{h}\sum_{n=2}^{M_l-1}\left(u^n-u^{n-1}\right)\left(v^n-v^{n-1}\right)+\frac{1}{h}\sum_{n=M_l+2}^{M-1}\left(u^n-u^{n-1}\right)\left(v^n-v^{n-1}\right)$$
$$+\sum_{n=M_l+1}^{M-1}u^nv^nh+\left(u^{M_l}-u^{M_l-1}\right)\left(v^{M_l-1}-v^{M_l}\right)+u^{M-1}v^{M-1}$$
$$+\left(u^{M_l+1}-u^{M_l}\right)\left(v^{M_l+1}-v^{M_l}\right).$$

Then $\left\langle A_hu^h,v^h\right\rangle=\left\langle u^h,A_hv^h\right\rangle$. So $A_h=A_h^*$. Moreover, using equality (2.2), we can write that

$$\left\langle A_hu^h,u^h\right\rangle = \frac{1}{h}\sum_{n=2}^{M_l-1}\left(u^n-u^{n-1}\right)\left(u^n-u^{n-1}\right)+\frac{1}{h}\sum_{n=M_l+2}^{M-1}\left(u^n-u^{n-1}\right)\left(u^n-u^{n-1}\right)$$
$$+\sum_{n=M_l+1}^{M-1}u^nu^nh+\left(u^{M_l}-u^{M_l-1}\right)\left(u^{M_l-1}-u^{M_l}\right)+u^{M-1}u^{M-1}$$
$$+\left(u^{M_l+1}-u^{M_l}\right)\left(u^{M_l+1}-u^{M_l}\right)$$

$$= \frac{2}{h}\sum_{n=2}^{M_l-1}\left(u^n-u^{n-1}\right)^2+\sum_{n=M_l+1}^{M-1}\left(u^n\right)^2h+\left(u^{M_l}-u^{M_l-1}\right)^2$$

$$+(u^{M_l+1}-u^{M_l})^2+\left(u^{M-1}\right)^2\geq 0.$$

So A_h is the positive operator.

CHAPTER 3

FIRST AND SECOND ORDER OF ACCURACY DIFFERENCE SCHEMES

3.1. Difference Schemes

$$\begin{cases} \frac{\partial u(t,x)}{\partial t} = \frac{\partial}{\partial x}(a(t,x)\frac{\partial u(t,x)}{\partial x}) + f(t,x), x \in (0,l), \\ \\ \frac{\partial u(t,x)}{\partial t} = \frac{\partial}{\partial x}(a(t,x)\frac{\partial u(t,x)}{\partial x}) + b(t,x)u(t,x) + g(t,x), x \in (l,L), \\ \\ t \in (0,T], u(0,x) = \varphi(x), x \in [0,L], \\ \\ u_x(t,0) = 0, u(t,L) = 0, t \in [0,T], \\ \\ u(t,l+) = u(t,l-), u_x(t,l+) = u_x(t,l-), t \in [0,T], \end{cases} \tag{3.1}$$

where $a(t,x)$, $b(t,x)$, $f(t,x)$, $g(t,x)$ and $\varphi(x)$ are given sufficiently smooth functions and $a(t,x) \geqslant 0$.

The discretization of problem (3.1) is carried out in two steps. In the first step let us define the grid spaces as,

$$[0,L]_h = \left\{ x_m = \begin{pmatrix} h_0 m, 0 \leq m \leq M_l, M_l h_0 = l, \\ \\ l + (m - M_l)h, M_l < m \leq M, (M - M_l)h = L - l. \end{pmatrix} \right\}$$

We introduce the Hilbert spaces $L_h = L_{[0,L]_h}$ of grid functions $u^h(x) = \{u_n\}_1^{M-1}$

defined on $[0, L]_h$, equipped with the norms

$$\| \varphi^h \|_{L_{[0,L]_h}} = \left(\sum_{n=1}^{M_l} |\varphi_n|^2 h_0 + \sum_{n=M_l+1}^{M-1} |\varphi_n|^2 h \right)^{\frac{1}{2}}.$$

To the differential operators $A^x(t)$ generated by the problem (3.1) for every fixed $t \in [0, T]$ we assign the first-order (second-order) of approximation of difference operators $A_h^x(t)$ acting in the space of grid functions $u^h(t, x) = \{u^n(t)\}_0^M$ satisfying the conditions $u^0(t) = u^1(t)(-u^2(t) + 4u^1(t) - 3u^0(t) = 0), u^M(t) = 0\}$by the formula

$$A_h^x(t)u^h = \left\{ \begin{array}{l} -\frac{1}{h_0}\left[a^{n+1}(t)\frac{u^{n+1}-u^n}{h_0} - a^n(t)\frac{u^n-u^{n-1}}{h_0}\right] + \sigma u^n, \\ \\ a^n = a(t, x_n), x_n = nh_0, 1 \le n \le M_l - 1, \\ \\ -u^{M_l}(t) + 4u^{M_l-1}(t) - 3u^{M_l-2}(t) \\ \\ = \frac{h_0}{h}\left[u^{M_l}(t) - 4u^{M_l+1}(t) + 3u^{M_l+2}(t)\right], \\ \\ -\frac{1}{h}\left[a^{n+1}(t)\frac{u^{n+1}-u^n}{h} - a^n(t)\frac{u^n-u^{n-1}}{h}\right] + \sigma u^n, \\ \\ a^n = a(t, x_n), x_n = l + (n - M_l)h, M_l + 1 \le n \le M - 1 \end{array} \right\}_{n=1}^{M-1}. \quad (3.2)$$

For every fixed $t \in [0, T]$ we introduce the difference operators $B_h^x(t)$ acting in the space of grid functions $u^h(t, x) = \{u^n(t)\}_0^M$ satisfying the conditions $u^0(t) = u^1(t)(-u^2(t) + 4u^1(t) - 3u^0(t) = 0), u^M(t) = 0$ by the formula

$$B_h^x(t)u^h = \left\{ \begin{array}{c} -\sigma u^n, 1 \le n \le M_l, \\ \\ -(\sigma - b^n(t))u^n, b^n(t) = b(t, x_n), \\ \\ x_n = l + (n - M_l)h, M_l + 1 \le n \le M - 1 \end{array} \right\}_{n=1}^{M-1}. \tag{3.3}$$

Here σ is a positive constant.

With the help of $A_h^x(t)$ and $B_h^x(t)$ we arrive at the initial- value problem

$$\left\{ \begin{array}{l} \frac{du^h(t)}{dt} + A_h^x(t)u^h(t) + B_h^x(t)u^h(t) = F^h(t), x \in [0, L]_h, t \in (0, T], \\ \\ u^h(0) = \varphi^h(x), \varphi^h(x) = \varphi(x), x \in [0, L]_h, \end{array} \right. \tag{3.4}$$

where

$$F^h(t) = \left\{ \begin{array}{c} f^h(t) = f(t, x_n), x_n = nh_0, 1 \le n \le M_l - 1, \\ \\ 0, \\ \\ g^h(t) = g(t, x_n), x_n = l + (n - M_l)h, M_l + 1 \le n \le M - 1 \end{array} \right\}_{n=1}^{M-1}.$$

In the second step we replace problem (3.4) by the difference schemes

$$\begin{cases} \frac{u_k^h(x)-u_{k-1}^h(x)}{\tau} + A_h^x(t_k)u_k^h(x) + B_h^x(t_k)u_k^h(x) = \varphi_k^h(x), \\ \varphi_k^h(x) = F^h(t_k, x), t_k = k\tau, \\ 1 \le k \le N, N\tau = T, u_0^h(x) = \varphi^h(x), x \in [0, L]_h, \end{cases} \tag{3.5}$$

$$\begin{cases} \frac{u_k^h(x)-u_{k-1}^h(x)}{\tau} + \frac{A_h^x(t_k-\frac{\tau}{2})}{2}\left(u_k^h(x) + u_{k-1}^h(x)\right) \\ +\frac{B_h^x(t_k-\frac{\tau}{2})}{2}\left(u_k^h(x) + u_{k-1}^h(x)\right) = \varphi_k^h(x), \\ \varphi_k^h(x) = F^h(t_k - \frac{\tau}{2}, x), t_k = k\tau, 1 \le k \le N, N\tau = T, \\ u_0^h(x) = \varphi^h(x), x \in [0, L]_h. \end{cases} \tag{3.6}$$

Theorem 3.1.1. The solutions of the difference schemes (3.5) and (3.6) satisfy the stability estimates:

$$\max_{1\le k\le N} \parallel u_k^h \parallel_{L_{[0,L]_{2h}}} \le C[||\varphi^h||_{L_{[0,L]_{2h}}} + \max_{1\le k\le N} \parallel {\varphi_k}^h \parallel_{L_{[0,L]_{2h}}}],$$

where C does not depend on $\varphi_k^h, 1 \le k \le N$,$\varphi^h$, h_0, h and τ.

Theorem 3.1.2. The solution of the difference scheme (3.5) satisfies the almost

coercive stability estimates:

$$\max_{1\le k\le N} \| \frac{u_k^h - u_{k-1}^h}{\tau} \|_{L_{2h}} \le C[||A_h^x(0)\varphi^h||_{L_{2h}} + \ln\frac{1}{\tau+h} \max_{1\le k\le N} \| \varphi_k{}^h \|_{L_{2h}}],$$

where C does not depend on $\varphi_k^h, 1 \le k \le N$,$\varphi^h$, h_0, h and τ.

Theorem 3.1.3. The solution of the difference scheme (3.6) satisfies the coercive stability estimates:

$$\left(\sum_{k=1}^{N} \| \frac{u_k^h - u_{k-1}^h}{\tau} \|_{L_{2h}}^2 \tau\right)^{\frac{1}{2}} \le C\left[||A_h^x(0)\varphi^h||_{L_{2h}} + \left(\sum_{k=1}^{N} \| \varphi_k{}^h \|_{L_{2h}}^2 \tau\right)^{\frac{1}{2}}\right],$$

where C does not depend on $\varphi_k^h, 1 \le k \le N$,$\varphi^h$, h_0, h and τ.

Proof of Theorem 3.1.1. The proof of this theorem is based on the discrete analogies of integral inequality and on the following formulas.

$$u_k^h = u_h(k,0)\varphi^h + \sum_{j=1}^{k} u_h(k,j)C_h^j \left\{-B_h^x(t_j)u_j^h + \varphi_j^h\right\}\tau, \tag{3.7}$$

$$k = 1, \cdots, N.$$

Here

$$u_h(k,j) = \begin{cases} R_h^k R_h^{k-1} \cdots R_h^{j+1} \text{ for } k \ne j, \\ \\ I \quad \text{for } k = j, \end{cases}$$

$$R_h^k = (I + \tau A_h^x(t_k))^{-1},$$
$$C_h^k = (I + \tau A_h^x(t_k))^{-1}$$

with the estimates

$$||u_h(k,j)|| \leq 1, ||C_h^k|| \leq 1, ||B_h^x(t)|| \leq C_1.$$

From (3.7) and the triangle inequality, it follows that

$$\left\|u_k^h\right\|_H = \|u_h(k,0)\|_{H\to H} \left\|\varphi^h\right\|_H + \sum_{j=1}^{k} \|u_h(k,j)\|_{H\to H}$$
$$\times \left\|C_h^j\right\|_{H\to H} \left\{\|B_h^x(t_j)\|_{H\to H} \left\|u_j^h\right\|_H + \left\|\varphi_j^h\right\|_H\right\} \tau$$

$$\leq \left\|\varphi^h\right\|_H + \sum_{j=1}^{k} \left\{C_1 \left\|u_j^h\right\|_H + \left\|\varphi_j^h\right\|_H\right\} \tau$$

So,

$$\left\|u_k^h\right\|_H \leq \left\|\varphi^h\right\|_H + \max_{1\leq j\leq N} \left\|\varphi_j^h\right\|_H k\tau + \sum_{j=1}^{k} C_1 \left\|u_j^h\right\|_H \tau$$

$$\leq \left\|\varphi^h\right\|_H + \max_{1\leq j\leq N} \left\|\varphi_j^h\right\|_H + C_1 \left\|u_k^h\right\|_H \tau$$

$$+ \sum_{j=1}^{k-1} C_1 \left\|u_j^h\right\|_H \tau.$$

Then,

$$(1 - C_1\tau) \left\|u_k^h\right\|_H \le \left\|\varphi^h\right\|_H + \max_{1\le j\le N} \left\|\varphi_j^h\right\|_H + \sum_{j=1}^{k-1} C_1 \left\|u_j^h\right\|_H \tau,$$

$$\left\|u_k^h\right\|_H = \frac{\left\|\varphi^h\right\|_H + \max\limits_{1\le j\le N} \left\|\varphi_j^h\right\|_H}{(1 - C_1\tau)} + C_2 \sum_{j=1}^{k-1} \left\|u_j^h\right\|_H \tau.$$

So

$$\left\|u_k^h\right\|_H = \frac{\left\|\varphi^h\right\|_H + \max\limits_{1\le j\le N} \left\|\varphi_j^h\right\|_H}{(1 - C_1\tau)} e^{C_2\tau k}.$$

In the same manner we can prove the theorem for the solution of difference scheme (3.6).

$$u_k^h = u_h(k,0)\varphi^h + \sum_{j=1}^{k} u_h(k,j) C_h^j \tag{3.8}$$

$$\times \left\{ -\frac{B_h^x(t_j - \frac{\tau}{2})}{2} \left(u_j^h(x) + u_{j-1}^h(x)\right) + \varphi_j^h \right\} \tau, k = 1, \cdots, N$$

Here

$$u_h(k,j) = \begin{cases} R_h^k R_h^{k-1} \cdots R_h^{j+1} \text{ for } k \ne j, \\ \\ I \quad \text{for } k = j, \end{cases}$$

where

$$R_h^k = \left(I - \frac{\tau A_h^x(t_k - \frac{\tau}{2})}{2}\right)\left(I + \frac{\tau A_h^x(t_k - \frac{\tau}{2})}{2}\right)^{-1},$$
$$C_h^k = \left(I + \frac{\tau A_h^x(t_k - \frac{\tau}{2})}{2}\right)^{-1}.$$

The proof of Theorem 3.1.2 and 3.1.3 is also based on the discrete analogies of integral inequality.

Note that, stability estimates could be also proved for the more general Pade difference schemes of the high order of accuracy generated by an exact difference scheme or by the Taylor's decomposition on the two points for the numerical solutions of this problem (see [Ashyralyev A. and Sobolevskii P.E.,2004]−[Ashiraliev A.and Sobolevskii P.E.,1988]).

3.2. Numerical Analysis

For numerical analysis we consider the initial-boundary value problem

$$\begin{cases} \frac{\partial u(t,x)}{\partial t} - \frac{\partial}{\partial x}(x\frac{\partial u(t,x)}{\partial x}) = f(t,x), 0 < t < 1,\ 0 < x < l, \\ \frac{\partial u(t,x)}{\partial t} - \frac{\partial}{\partial x}(x\frac{\partial u(t,x)}{\partial x}) + u(t,x) = g(t,x),\ 0 < t < 1,\ l < x < \pi, \\ u(0,x) = \varphi(x), \varphi(x) = \cos\frac{x}{2},\quad 0 \le x \le \pi, \\ u_x(t,0) = u(t,\pi) = 0, u(t,l+) = u(t,l-)\quad , \\ u_x(t,l+) = u_x(t,l-)\ \ 0 \le t \le 1. \end{cases} \tag{3.9}$$

where

$$f(t,x)=\frac{1}{2}\exp(\frac{-t}{2})(\frac{x-2}{2}\cos\frac{x}{2}+\sin\frac{x}{2})$$

and

$$g(t,x)=\frac{1}{2}\exp(\frac{-t}{2})(\frac{x+2}{2}\cos\frac{x}{2}+\sin\frac{x}{2}).$$

The exact solution of (3.9) is

$$u\left(t,x\right)=e^{-\frac{t}{2}}\cos\frac{x}{2}.$$

First, applying the first order of accuracy difference scheme (3.5), we present the following first order of accuracy difference scheme for the approximate solutions of the problem (3.9)

$$\begin{cases} \frac{u_n^k-u_n^{k-1}}{\tau}-\frac{1}{h_0}\left(x_{n+1}\frac{u_{n+1}^k-u_n^k}{h_0}-x_n\frac{u_n^k-u_{n-1}^k}{h_0}\right)=\varphi_n^k, \\ \varphi_n^k=f(t_k,x_n),\ t_k=k\tau,\ x_n=nh_0,1\le k\le N,1\le n\le M_l-1\ , \\ \frac{u_n^k-u_n^{k-1}}{\tau}-\frac{1}{h}\left(x_{n+1}\frac{u_{n+1}^k-u_n^k}{h}-x_n\frac{u_n^k-u_{n-1}^k}{h}\right)+u_n^k=\varphi_n^k, \\ \varphi_n^k=g(t_k,x_n),t_k=k\tau,\ x_n=l+(n-M_l)h,1\le k\le N,M_l+1\le n\le M-1\ , \\ u_n^0=\varphi(x_n),\ x_n=h_0n,0\le n\le M_l;x_n=l+(n-M_l)h,M_l+1\le n\le M, \\ \frac{u_1^k-u_0^k}{h_0}=u_M^k=0,\quad 0\le k\le N, \\ h_0\left(u_{M_l+1}^k-u_{M_l}^k\right)=h\left(u_{M_l}^k-u_{M_l-1}^k\right),0\le k\le N. \end{cases} \tag{3.10}$$

We have $(M+1)\times(M+1)$ system of linear equations in (3.10) and we write them in the matrix form

$$A\,U^k + B\,U^{k-1} = R\varphi^k, \quad 1 \le k \le N,\ U^0 = \varphi\ , \tag{3.11}$$

where

$$A = \begin{bmatrix}
1 & -1 & 0 & . & 0 & 0 & 0 & 0 & 0 & . & 0 \\
x_0 & y_0 & z_0 & . & 0 & 0 & 0 & 0 & 0 & . & 0 \\
0 & x_1 & y_1 & . & 0 & 0 & 0 & 0 & 0 & . & 0 \\
. & . & . & . & . & . & . & . & . & . & . \\
0 & 0 & 0 & . & x_{M_l-1} & y_{M_l-1} & z_{M_l-1} & 0 & 0 & . & 0 \\
0 & 0 & 0 & . & 0 & h & -(h+h_0) & h_0 & 0 & . & 0 \\
0 & 0 & 0 & . & 0 & 0 & x_{M_l+1} & y_{M_l+1} & z_{M_l+1} & . & 0 \\
0 & 0 & 0 & . & 0 & 0 & 0 & x_{M_l+2} & y_{M_l+2} & . & 0 \\
. & . & . & . & . & . & . & . & . & . & . \\
0 & 0 & 0 & . & 0 & 0 & 0 & 0 & 0 & . & z_{M-1} \\
0 & 0 & 0 & . & 0 & 0 & 0 & 0 & 0 & . & 1
\end{bmatrix},$$

$$B = \begin{bmatrix} 0 & 0 & 0 & 0 & 0 & . & 0 & 0 & 0 \\ 0 & v & 0 & 0 & 0 & . & 0 & 0 & 0 \\ 0 & 0 & v & 0 & 0 & . & 0 & 0 & 0 \\ . & . & . & . & . & . & . & . & . \\ 0 & 0 & 0 & 0 & 0 & . & 0 & 0 & 0 \\ 0 & 0 & 0 & 0 & 0 & . & v & 0 & 0 \\ 0 & 0 & 0 & 0 & 0 & . & 0 & v & 0 \\ 0 & 0 & 0 & 0 & 0 & . & 0 & 0 & 0 \end{bmatrix},$$

Here

$$x_n = \begin{cases} -\frac{n}{h_0}, & 0 \le n \le M_l - 1 \ , \\ \\ -\frac{l+(n-M_l)h}{h^2}, & M_l + 1 \le n \le M - 1, \end{cases}$$

$$z_n = \begin{cases} -\frac{n+1}{h_0}, & 0 \le n \le M_l - 1 \ , \\ \\ -\frac{l+(n-M_l+1)h}{h^2}, & M_l + 1 \le n \le M - 1, \end{cases}$$

$$y_n = \begin{cases} \frac{1}{\tau} + \frac{2n+1}{2h_0}, & 0 \le n \le M_l - 1 \ , \\ \\ \frac{1}{\tau} + \frac{2l+(2n-2M_l+1)h}{h^2} + 1, & M_l + 1 \le n \le M - 1, \end{cases}$$

$$v = -\frac{1}{\tau}.$$

$$U^s = \begin{bmatrix} U_0^s \\ ... \\ U_M^s \end{bmatrix} \quad for\ s = k, k-1\ and\ \varphi = \begin{bmatrix} \varphi_{(x_0)} \\ ... \\ \varphi(x_M) \end{bmatrix},$$

$$R = \begin{bmatrix} 1 & 0 & . & 0 \\ 0 & 1 & . & 0 \\ . & . & . & . \\ 0 & 0 & . & 1 \end{bmatrix}, \quad \varphi^k = \begin{bmatrix} 0 \\ \varphi_1^k \\ ... \\ \varphi_{M_l-1}^k \\ 0 \\ \varphi_{M_l+1}^k \\ ... \\ \varphi_{M-1}^k \\ 0 \end{bmatrix}.$$

So, we have the first order difference equation with respect to k with matrix coefficients. From (3.11) it follows that

$$U^k = -A^{-1}BU^{k-1} + A^{-1}R\varphi^k \quad k = 1, \cdots, N. \tag{3.12}$$

Second, applying the second order of accuracy difference scheme (3.6), we present the following second order of accuracy difference scheme for the approximate solutions of

the problem (3.9)

$$
\begin{cases}
\frac{u_n^k-u_n^{k-1}}{\tau}-\frac{1}{2h_0}\left(x_{n+1}\frac{u_{n+1}^k-u_n^k}{h_0}-x_n\frac{u_n^k-u_{n-1}^k}{h_0}\right) \\
-\frac{1}{2h_0}\left(x_{n+1}\frac{u_{n+1}^{k-1}-u_n^{k-1}}{h_0}-x_n\frac{u_n^{k-1}-u_{n-1}^{k-1}}{h_0}\right)=\varphi_n^k, \varphi_n^k=f(t_k-\frac{\tau}{2},x_n), \\
t_k=k\tau,\ x_n=nh_0, 1\le k\le N, 1\le n\le M_l-1\ , \\
\frac{u_n^k-u_n^{k-1}}{\tau}-\frac{1}{2h}\left(x_{n+1}\frac{u_{n+1}^k-u_n^k}{h}-x_n\frac{u_n^k-u_{n-1}^k}{h}\right) \\
-\frac{1}{2h}\left(x_{n+1}\frac{u_{n+1}^{k-1}-u_n^{k-1}}{h}-x_n\frac{u_n^{k-1}-u_{n-1}^{k-1}}{h}\right)+\frac{1}{2}\left\{u_n^k+u_n^{k-1}\right\}=\varphi_n^k, \\
\varphi_n^k=g(t_k-\frac{\tau}{2},x_n), t_k=k\tau,\ x_n=l+(n-M_l)h, 1\le k\le N, M_l+1\le n\le M-1\ , \\
u_n^0=\varphi(x_n),\ x_n=h_0n, 0\le n\le M_l; x_n=l+(n-M_l)h, M_l+1\le n\le M, \\
-u_2^k+4u_1^k-3u_0^k=u_M^k=0,\quad 0\le k\le N, \\
h_0\left(-u_{M_l+2}^k+4u_{M_l+1}^k-3u_{M_l}^k\right) \\
=h\left(u_{M_l-2}^k-4u_{M_l-1}^k+3u_{M_l}^k\right), 0\le k\le N.
\end{cases}
\tag{3.13}
$$

We have again $(M+1)\times(M+1)$ system of linear equations and we write them in the matrix form (3.11), where

$$A = \begin{bmatrix} 3 & 4 & -1 & . & 0 & 0 & 0 & 0 & . & 0 \\ x_0 & y_0 & z_0 & . & 0 & 0 & 0 & 0 & . & 0 \\ 0 & x_1 & y_1 & . & 0 & 0 & 0 & 0 & . & 0 \\ .. & .. & .. & . & .... & ... & ... & ... & . & . \\ 0 & 0 & 0 & . & y_{_{M_l-1}} & z_{M_l-1} & 0 & 0 & . & 0 \\ 0 & 0 & 0 & . & 4h & -3(h+h_0) & 4h_0 & -h_0 & . & 0 \\ 0 & 0 & 0 & . & 0 & x_{M_l+1} & y_{M_l+1} & z_{_{M_l+1}} & . & 0 \\ 0 & 0 & 0 & . & 0 & 0 & x_{M_l+2} & y_{M_l+2} & . & 0 \\ .. & .. & .. & . & ... & ... & ... & ... & . & . \\ 0 & 0 & 0 & . & 0 & 0 & 0 & 0 & . & z_{M-1} \\ 0 & 0 & 0 & . & 0 & 0 & 0 & 0 & . & 1 \end{bmatrix},$$

$$B = \begin{bmatrix} 0 & 0 & 0 & . & 0 & 0 & 0 & . & 0 \\ x_0 & q_0 & z_0 & . & 0 & 0 & 0 & . & 0 \\ 0 & x_1 & q_1 & . & 0 & 0 & 0 & . & 0 \\ . & . & . & . & . & . & . & . & . \\ 0 & 0 & 0 & . & z_{M_l-1} & 0 & 0 & . & 0 \\ 0 & 0 & 0 & . & 0 & 0 & 0 & . & 0 \\ 0 & 0 & 0 & . & x_{M_l+1} & q_{M_l+1} & z_{M_l+1} & . & 0 \\ . & . & . & . & . & . & . & . & . \\ 0 & 0 & 0 & . & 0 & 0 & 0 & . & z_{M-1} \\ 0 & 0 & 0 & . & 0 & 0 & 0 & . & 0 \end{bmatrix},$$

Here

$$x_n = \begin{cases} -\frac{n}{2h_0}, & 0 \le n \le M_l - 1 \ , \\ \\ -\frac{l+(n-M_l)h}{2h^2}, & M_l + 1 \le n \le M - 1, \end{cases}$$

$$z_n = \begin{cases} -\frac{n+1}{2h_0}, & 0 \le n \le M_l - 1 \ , \\ \\ -\frac{l+(n-M_l+1)h}{2h^2}, & M_l + 1 \le n \le M - 1, \end{cases}$$

$$y_n = \begin{cases} \frac{1}{\tau} + \frac{2n+1}{2h_0}, & 0 \le n \le M_l - 1 \ , \\ \\ \frac{1}{\tau} + \frac{2l+(2n-2M_l+1)h}{2h^2} + \frac{1}{2}, & M_l + 1 \le n \le M - 1, \end{cases}$$

$$q_n = \begin{cases} -\frac{1}{\tau} + \frac{2n+1}{2h_0}, & 0 \le n \le M_l - 1 \ , \\ \\ -\frac{1}{\tau} + \frac{2l+(2n-2M_l+1)h}{2h^2} + \frac{1}{2}, & M_l + 1 \le n \le M - 1. \end{cases}$$

Now, we will give the results of the numerical analysis.In order to get the solution of (3.10) and (3.13) we use (3.12) and MATLAB programs. The numerical solutions are recorded for different values of $N = M$, M_l and u_n^k represents the numerical solutions of these difference schemes at (t_k, x_n). First, for their comparison, the errors computed by

$$E = \max_{\substack{1\leq k\leq N \\ 1\leq n\leq M}} \left| u(t_k, x_n) - u_n^k \right|.$$

Tables 1 and 2 give the error analysis between the exact solution and solutions derived by difference schemes. Table 1 is constructed for $h = h_0 = \frac{\pi}{M}$ and $N = M = 20$, 40 and 60 respectively, when M_l is $\frac{9M}{10}$ or $\frac{13M}{20}$.

Table 1. Numerical analysis for $h = h_0$

Method	N=M=20	N=M=40	N=M=60
1^{st} order of accuracy ($\frac{13M}{20}$)	0.0158	0.0082	0.0056
1^{st} order of accuracy ($\frac{9M}{10}$)	0.0178	0.0091	0.0061
2^{nd} order of accuracy ($\frac{13M}{20}$)	$9.2142.10^{-5}$	$2.5762.10^{-5}$	$1.1862.10^{-5}$
2^{nd} order of accuracy ($\frac{9M}{10}$)	$1.0734.10^{-4}$	$2.7111.10^{-5}$	$1.2088.10^{-5}$

Table 2 is constructed for $h = 0.01$ and $N = M = 20$, 40 and 60 respectively, when $M_l = \frac{9M}{10}$ or $M_l = \frac{13M}{20}$, we can obtain $h_0 = (\pi - h(M - M_l))/M_l$.

Table 2. Numerical analysis for different h and h_0

Method	N=M=20	N=M=40	N=M=60
1^{st} order of accuracy $(\frac{13M}{20})$	0.0245	0.0124	0.0081
1^{st} order of accuracy $(\frac{9M}{10})$	0.0193	0.0098	0.0066
2^{nd} order of accuracy $(\frac{13M}{20})$	$4.0302.10^{-4}$	$1.1098.10^{-4}$	$5.3\ .10^{-5}$
2^{nd} order of accuracy $(\frac{9M}{10})$	$1.5804.10^{-4}$	$4.1352.10^{-5}$	$1.9128.10^{-5}$

Second, for their comparison, the errors computed by

$$E = \max_{1\leq k\leq N} \left\{ \sum_{n=1}^{M_l} \left|u(t_k, x_n) - u_n^k\right|^2 h_0 + \sum_{n=M_l+1}^{M} \left|u(t_k, x_n) - u_n^k\right|^2 h \right\}^{\frac{1}{2}}$$

and the Table 3 is constructed for $h = h_0 = \frac{\pi}{M}$ and $N = M = 20$, 40 and 60 respectively, when M_l is $\frac{9M}{10}$ or $\frac{13M}{20}$.

Table 3. Numerical analysis for $h = h_0$

Method	N=M=20	N=M=40	N=M=60
1^{st} order of accuracy $(\frac{13M}{20})$	0.0193	0.0099	0.0066
1^{st} order of accuracy $(\frac{9M}{10})$	0,0209	0,0105	0,007
2^{nd} order of accuracy $(\frac{13M}{20})$	$2.0841.10^{-6}$	$6.4106.10^{-7}$	$3.0643.10^{-7}$
2^{nd} order of accuracy $(\frac{9M}{10})$	$2.7907.10^{-6}$	$6.9214.10^{-7}$	$3.0643.10^{-7}$

Table 4 is constructed for $h = 0.01$ and $N = M = 20$, 40 and 60 respectively, when $M_l = \frac{9M}{10}$ or $M_l = \frac{13M}{20}$, we can obtain $h_0 = (\pi - h(M - M_l))/M_l$.

Table 4. Numerical analysis for different h and h_0

Method	N=M=20	N=M=40	N=M=60
1^{st} order of accuracy $(\frac{13M}{20})$	0,0073	0,0051	0,0041
1^{st} order of accuracy $(\frac{9M}{10})$	0.0057	0.004	0.0033
2^{nd} order of accuracy $(\frac{13M}{20})$	$3.5428.10^{-5}$	$1.111.10^{-5}$	$6.1807.10^{-6}$
2^{nd} order of accuracy $(\frac{9M}{10})$	$5.7752.10^{-6}$	$1.5593.10^{-6}$	$7.5472.10^{-7}$

Thus, the second order of accuracy difference schemes are more accurate comparing with the first order of accuracy difference scheme.

CHAPTER 4

R-MODIFIED CRANK-NICHOLSON DIFFERENCE SCHEME

4.1. Difference Schemes

We consider again the problem (3.1). It is known that (*see* [Ashyralyev A.,1989], [Luskin M. and Rannacher R.,1982] and [Rannacher R.,1982]) the Crank-Nicholson difference scheme (3.6) is not convergent for unsmooth datas. Therefore, in this chapter we will consider the r-modified Crank-Nicholson difference schemes for the numerical solution of (3.1). The discretization of problem (3.1) is carried out also in two steps. In the first step, we consider the same discretization in x given in the previous chapter.In the second step, applying the modified Crank-Nicholson difference schemes of papers [Ashyralyev A.,1989], [Luskin M. and Rannacher R.,1982] and [Rannacher R.,1982], we get

$$
\begin{cases}
\frac{u_k^h(x)-u_{k-1}^h(x)}{\tau}+A_h^x(t_k-\frac{\tau}{2})u_k^h(x)+B_h^x(t_k-\frac{\tau}{2})u_k^h(x)=\varphi_k^h(x), \\
\varphi_k^h(x)=F^h(t_k-\frac{\tau}{2},x), t_k=k\tau, \\
1\le k\le r, N\tau=T, u_0^h(x)=\varphi^h(x), x\in[0,L]_h, \\
\\
\frac{u_k^h(x)-u_{k-1}^h(x)}{\tau}+\frac{A_h^x(t_k-\frac{\tau}{2})}{2}\left(u_k^h(x)+u_{k-1}^h(x)\right) \\
+\frac{B_h^x(t_k-\frac{\tau}{2})}{2}\left(u_k^h(x)+u_{k-1}^h(x)\right)=\varphi_k^h(x), \\
\varphi_k^h(x)=F^h(t_k-\frac{\tau}{2},x), t_k=k\tau, r+1\le k\le N, N\tau=T, \\
\\
u_0^h(x)=\varphi^h(x), x\in[0,L]_h.
\end{cases}
\tag{4.1}
$$

Theorem 4.1.1. The solution of the difference scheme (4.1) satisfies the stability estimates:

$$\max_{1\le k\le N} \| u_k^h \|_{L_{2h}} \le C[||\varphi^h||_{L_{2h}} + \max_{1\le k\le N} \| \varphi_k{}^h \|_{L_{2h}}],$$

where C does not depend on $\varphi_k^h, 1 \le k \le N, \varphi^h$, h_0, h and τ.

Theorem 4.1.2. The solution of the difference scheme (4.1) satisfies the almost coercive stability estimates:

$$\max_{1\le k\le N} \| \frac{u_k^h - u_{k-1}^h}{\tau} \|_{L_{2h}} \le C[||A_h^x(0)\varphi^h||_{L_{2h}} + \ln\frac{1}{\tau+h} \max_{1\le k\le N} \| \varphi_k{}^h \|_{L_{2h}}],$$

where C does not depend on $\varphi_k^h, 1 \le k \le N, \varphi^h$, h_0, h and τ.

Theorem 4.1.3. The solution of the difference scheme (4.1) satisfies the coercive stability estimates:

$$\left(\sum_{k=1}^{N} \| \frac{u_k^h - u_{k-1}^h}{\tau} \|_{L_{2h}}^2 \tau\right)^{\frac{1}{2}} \le C\left[||A_h^x(0)\varphi^h||_{L_{2h}} + \left(\sum_{k=1}^{N} \| \varphi_k{}^h \|_{L_{2h}}^2 \tau\right)^{\frac{1}{2}}\right],$$

where C does not depend on $\varphi_k^h, 1 \le k \le N, \varphi^h$, h_0, h and τ.

Proof. The proof of these theorems is based on the discrete analogies of integral inequality and on the following formulas

$$u_k^h = u_h(k,0)\varphi^h + \sum_{j=1}^{k} u_h(k,j)C_h^j \left\{-B_h^x(t_j - \frac{\tau}{2})u_j^h + \varphi_j^h\right\}\tau, \tag{4.2}$$

$$k = 1, \cdots, r,$$

$$u_k^h = u_h(k,0)\varphi^h + \sum_{j=1}^{k} u_h(k,j)C_h^j \tag{4.3}$$

$$\times \left\{ -\frac{B_h^x(t_j - \frac{\tau}{2})}{2}\left(u_j^h(x) + u_{j-1}^h(x)\right) + \varphi_j^h \right\} \tau, k = r+1, \cdots, N$$

for the solution of difference scheme (4.1) and on the estimates

$$||u_h(k,j)|| \le 1, ||C_h^k|| \le 1, ||B_h^x(t_k - \frac{\tau}{2})|| \le C_2.$$

Here

$$u_h(k,j) = \begin{cases} R_h^k \cdots R_h^{j+1} \text{ for } k \ne j, \\ \\ I \quad \text{for } k = j, \end{cases}$$

where

$$R_h^k = \begin{cases} \left(I + \tau A_h^x(t_k - \frac{\tau}{2})\right)^{-1} \ , \ 1 \le k \le r, \\ \\ \left(I - \frac{\tau A_h^x(t_k - \frac{\tau}{2})}{2}\right)\left(I + \frac{\tau A_h^x(t_k - \frac{\tau}{2})}{2}\right)^{-1}, \ r+1 \le k \le N \end{cases}$$

and

$$C_h^k = \begin{cases} \left(I + \tau A_h^x(t_k - \frac{\tau}{2})\right)^{-1} \ , \ 1 \le k \le r, \\ \\ \left(I + \frac{\tau A_h^x(t_k - \frac{\tau}{2})}{2}\right)^{-1}, \ r+1 \le k \le N. \end{cases}$$

Note that, stability estimates could be also proved for the more general Pade difference schemes of the high order of accuracy generated by an exact difference scheme or by the Taylor's decomposition on the two points for the numerical solutions of this problem.

4.2. Numerical Analysis

For numerical analysis we consider the initial-boundary value problem

$$\begin{cases} \frac{\partial u(t,x)}{\partial t} - \frac{\partial^2 u(t,x)}{\partial x^2} = f(t,x), 0 < t < 1,\ 0 < x < l, \\ \frac{\partial u(t,x)}{\partial t} - \frac{\partial^2 u(t,x)}{\partial x^2} + u(t,x) = g(t,x), 0 < t < 1,\ l < x < 1, \\ u(0,x) = \varphi(x) = 0, 0 \le x \le 1, \\ u_x(t,0) = u(t,1) = 0, \\ u(t,l+) = u(t,l-)\ \ , u_x(t,l+) = u_x(t,l-),\ \ 0 \le t \le 1. \end{cases} \tag{4.4}$$

where

$$f(t,x) = \frac{1}{2}t^{-\frac{1}{2}}(x-x^2)^{\frac{5}{2}} - \frac{15}{4}t^{\frac{1}{2}}(x-x^2)^{\frac{3}{2}}(1-2x) + 5t^{\frac{1}{2}}(x-x^2)^{\frac{3}{2}},$$

$$g(t,x) = t^{\frac{1}{2}}(x-x^2)^{\frac{5}{2}} + \frac{1}{2}t^{-\frac{1}{2}}(x-x^2)^{\frac{5}{2}} - \frac{15}{4}t^{\frac{1}{2}}(x-x^2)^{\frac{3}{2}}(1-2x) + 5t^{\frac{1}{2}}(x-x^2)^{\frac{3}{2}}.$$

The exact solution of (4.4) is

$$u(t,x) = t^{\frac{1}{2}}(x-x^2)^{\frac{5}{2}}.$$

Applying the difference scheme (4.1), we present the following r-modified Crank-Nicholson difference scheme for the approximate solution of the initial-boundary value problem (4.4).

$$
\begin{cases}
\frac{u_n^k-u_n^{k-1}}{\tau}-\frac{u_{n+1}^k-2u_n^k+u_{n-1}^k}{h^2}=\varphi_n^k, \\
\\
\varphi_n^k=f(t_k-\frac{\tau}{2},x_n),\ t_k=k\tau,\ x_n=nh, \\
1\le k\le r, 1\le n\le M_l-1, \\
\\
\frac{u_n^k-u_n^{k-1}}{\tau}-\frac{u_{n+1}^k-2u_n^k+u_{n-1}^k}{h^2}+u_n^k=\varphi_n^k, \\
\\
\varphi_n^k=g(t_k-\frac{\tau}{2},x_n), t_k=k\tau,\ x_n=nh, \\
1\le k\le r, M_l+1\le n\le M-1, \\
\\
\frac{u_n^k-u_n^{k-1}}{\tau}-\frac{1}{2}\left\{\left(\frac{u_{n+1}^k-2u_n^k+u_{n-1}^k}{h^2}\right)+\left(\frac{u_{n+1}^{k-1}-2u_n^{k-1}+u_{n-1}^{k-1}}{h^2}\right)\right\}=\varphi_n^k, \\
\\
\varphi_n^k=f(t_k-\frac{\tau}{2},x_n), t_k=k\tau,\ x_n=nh, \\
r+1\le k\le N, 1\le n\le M_l-1\ , \\
\\
\frac{u_n^k-u_n^{k-1}}{\tau}-\frac{1}{2}\left\{\left(\frac{u_{n+1}^k-2u_n^k+u_{n-1}^k}{h^2}\right)+\left(\frac{u_{n+1}^{k-1}-2u_n^{k-1}+u_{n-1}^{k-1}}{h^2}\right)\right\} \\
+\frac{1}{2}\left\{u_n^k+u_n^{k-1}\right\}=\varphi_n^k, \\
\\
\varphi_n^k=g(t_k-\frac{\tau}{2},x_n), t_k=k\tau,\ x_n=nh, \\
r+1\le k\le N, M_l+1\le n\le M-1\ \ , \\
\\
u_n^0=0,\ 1\le n\le M \\
\\
-u_2^k+4u_1^k-3u_0^k=u_M^k=0,\ \ 0\le k\le N, \\
\\
\left(-u_{M_l+2}^k+4u_{M_l+1}^k-3u_{M_l}^k\right)=\left(u_{M_l-2}^k-4u_{M_l-1}^k+3u_{M_l}^k\right), \\
0\le k\le N.
\end{cases}
\tag{4.5}
$$

We have $(M+1)\times(M+1)$ system of linear equations in (4.5) and we write them in the matrix form

$$A\,U^k + B\,U^{k-1} = R\varphi^k, \quad 1 \le k \le N,\ U^0 = \varphi\ , \tag{4.6}$$

where

$$A = \begin{bmatrix} 3 & 4 & -1 & . & 0 & 0 & 0 & 0 & . & 0 \\ x_0 & y_0 & z_0 & . & 0 & 0 & 0 & 0 & . & 0 \\ 0 & x_1 & y_1 & . & 0 & 0 & 0 & 0 & . & 0 \\ .. & .. & .. & . & .... & ... & ... & ... & . & . \\ 0 & 0 & 0 & . & y_{M_l-1} & z_{M_l-1} & 0 & 0 & . & 0 \\ 0 & 0 & 0 & . & 4 & -6 & 4 & -1 & . & 0 \\ 0 & 0 & 0 & . & 0 & x_{M_l+1} & y_{M_l+1} & z_{M_l+1} & . & 0 \\ 0 & 0 & 0 & . & 0 & 0 & x_{M_l+2} & y_{M_l+2} & . & 0 \\ .. & .. & .. & . & ... & ... & ... & ... & . & . \\ 0 & 0 & 0 & . & 0 & 0 & 0 & 0 & . & z_{M-1} \\ 0 & 0 & 0 & . & 0 & 0 & 0 & 0 & . & 1 \end{bmatrix},$$

$$B = \begin{bmatrix} 0 & 0 & 0 & . & 0 & 0 & 0 & . & 0 \\ w_0 & q_0 & p_0 & . & 0 & 0 & 0 & . & 0 \\ 0 & w_1 & q_1 & . & 0 & 0 & 0 & . & 0 \\ . & . & . & . & . & . & . & . & . \\ 0 & 0 & 0 & . & p_{M_l-1} & 0 & 0 & . & 0 \\ 0 & 0 & 0 & . & 0 & 0 & 0 & . & 0 \\ 0 & 0 & 0 & . & w_{M_l+1} & q_{M_l+1} & p_{M_l+1} & . & 0 \\ . & . & . & . & . & . & . & . & . \\ 0 & 0 & 0 & . & 0 & 0 & 0 & . & p_{M-1} \\ 0 & 0 & 0 & . & 0 & 0 & 0 & . & 0 \end{bmatrix},$$

Here

$$x_n = \begin{cases} -\frac{n}{h}, & 0 \le n \le r \ , \\ \\ -\frac{n}{2h}, & r+1 \le n \le M-1 \ , \end{cases}$$

$$z_n = \begin{cases} -\frac{n+1}{h_0}, & 0 \le n \le r \ , \\ \\ -\frac{n+1}{2h_0}, & r+1 \le n \le M-1 \ , \end{cases}$$

$$y_n = \begin{cases} \frac{1}{\tau} + \frac{2n+1}{2h}, & 0 \le n \le M_l - 1 \ , \\ \\ \frac{1}{\tau} + \frac{2n+1}{2h} + \frac{1}{2}, & M_l + 1 \le n \le M-1, \end{cases}$$

$$w_n = \begin{cases} 0, \quad 0 \le n \le r \ , \\ \\ -\frac{n}{2h}, \quad r+1 \le n \le M-1 \ , \end{cases}$$

$$q_n = \begin{cases} -\frac{1}{\tau}, \quad 0 \le n \le r, \\ \\ -\frac{1}{\tau} + \frac{2n+1}{2h}, \quad r+1 \le n \le M_l - 1 \ , \\ \\ -\frac{1}{\tau} + \frac{2n+1}{2h} + \frac{1}{2}, \quad M_l + 1 \le n \le M-1, \end{cases}$$

$$p_n = \begin{cases} 0, \ 0 \le n \le r \ , \\ \\ -\frac{n+1}{2h}, \ r+1 \le n \le M-1, \end{cases}$$

$$U^s = \begin{bmatrix} U_0^s \\ ... \\ U_M^s \end{bmatrix} \quad for \ s = k, k-1 \ and \ \varphi = \begin{bmatrix} \varphi_{(x_0)} \\ ... \\ \varphi(x_M) \end{bmatrix} \ ,$$

$$R = \begin{bmatrix} 1 & 0 & . & 0 \\ 0 & 1 & . & 0 \\ . & . & . & . \\ 0 & 0 & . & 1 \end{bmatrix}, \quad \varphi^k = \begin{bmatrix} 0 \\ \varphi_1^k \\ \cdots \\ \varphi_{M_l-1}^k \\ 0 \\ \varphi_{M_l+1}^k \\ \cdots \\ \varphi_{M-1}^k \\ 0 \end{bmatrix}.$$

So, we have the first order difference equation with respect to k with matrix coefficients. From (4.6) it follows that

$$U^k = -A^{-1}BU^{k-1} + A^{-1}R\varphi^k \quad k = 1, \cdots, N. \tag{4.7}$$

Now, we will give the results of the numerical analysis.In order to get the solution of (4.5), we use (4.7) and MATLAB program. Numerical solutions are recorded for different values of $N = M$, M_l and u_n^k represents the numerical solution of r-modified Crank-Nicholson difference scheme at (t_k, x_n). For their comparison, the errors computed by

$$E = \max_{1 \le k \le N} \left\{ \sum_{n=1}^{M_l} \left| u(t_k, x_n) - u_n^k \right|^2 h_0 + \sum_{n=M_l+1}^{M} \left| u(t_k, x_n) - u_n^k \right|^2 h \right\}^{\frac{1}{2}}.$$

Table 5 gives the error analysis between the exact solution and solutions derived by

difference schemes. Table is constructed for $M_l = \frac{9M}{10}$ and $N = M = 20$, 40 respectively.

Table 5. Numerical analysis for-modified Crank-Nicholson

Method	N=M=20	N=M=40
1^{st} order of accuracy	0.12	0.1205
2^{nd} order of accuracy	1.0813x10^7	1.8024x10^5
2-modified Crank-Nicholson	0.0441	0.0272

Second, for their comparison, the errors computed by

$$E = \max \left\{ \sum_{n=1}^{M_l} \left| u(t_N, x_n) - u_n^N \right|^2 h_0 + \sum_{n=M_l+1}^{M} \left| u(t_N, x_n) - u_n^N \right|^2 h \right\}^{\frac{1}{2}}$$

and the Table 6 is constructed for $N = M = 20$ and 40 , when M_l is $\frac{9M}{10}$.

Table 6. Numerical analysis for end point for-modified Crank-Nicholson

Method	N=M=20	N=M=40
1^{st} order of accuracy	0.0139	0.0074
2^{nd} order of accuracy	$1.5122 \text{x} 10^{3}$	0.0086
2-modified Crank-Nicholson	0.0082	0.0046

CHAPTER 5

APPLICATIONS

5.1. A Brief Terminology for Biology

Atherosclerosis is a type of arteriosclerosis.It's the term for the process of fatty substances, cholesterol, cellular waste products, calcium and fibrin (a clotting material in the blood) building up in the inner lining of an artery. Arteriosclerosis is a general term for the thickening and hardening of arteries. Atherosclerosis is a slow, progressive disease that may start in childhood. Atherosclerosis affects large and medium-sized arteries. Complications of atherosclerosis include stroke or TIA in the brain, angina (chest pain), heart attack, kidney failure, erectile dysfunction and PAD (peripheral artery disease).

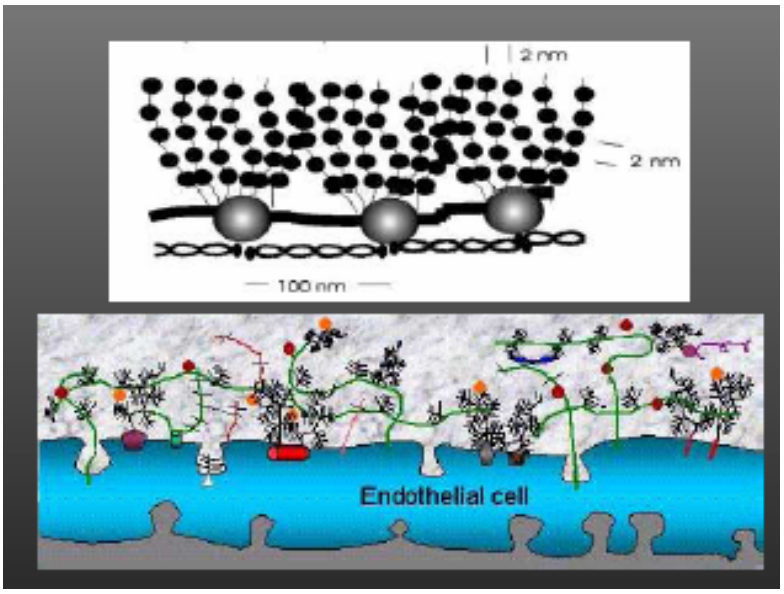

Figure 1. The structure of endothelial cell.

Endothelial cells are very flat, have a central nucleus, are about 1-2 μm thick and some 10-20 μm in diameter. They form flat, pavement-like patterns on the inside of the vessels and at the junctions between cells there are overlapping regions which help to seal the vessel.Endothelial cells are selective filters which regulate the passage of gases, fluid and various molecules across their cell membranes. Endothelial cells are also responsive to local agents such as histamine, which is released when local tissues are damaged. Consequently, the endothelial cells open up their intercellular junctions and allow the passage of large amounts of fluid from blood plasma so that the surrounding tissues become engorged with fluid and swollen: a condition called oedema. At the same time large numbers of leucocytes, escape and flood into the tissues. These events are the hallmarks of the inflammatory response. It is exemplified by a simple scratch on the skin or a splinter wound: the area quickly becomes reddened (opening up of capillaries) and swollen (oedema).

5.2. Methods

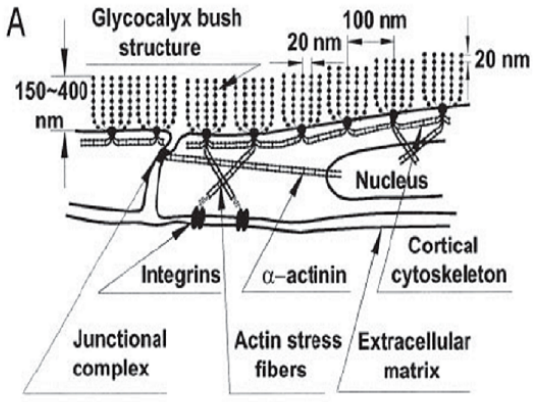

Figure 2. Surface of endothelial cells and glycocalyx inside the micro channels (Squire J.M., et all).

Surface of endothelial cells and glycocalyx bush structure inside the cardiovascular channels are illustrated in Figure 2 [Squire J.M., Chew M., Nneji G., Neal C., Barry J. and Michel C., 2001]. The schematic of the glycocalyx bush structure for computational modeling studies is illustrated in Figure 3. The structure of the single glycocalyx was assumed as a cylindrical shape. The diameter of the single glycoprotein in the glycocalyx is taken as 10 nm and the length of it is taken as 210 nm. The distance between glycoproteins in glycocalyx is assumed 20 nm. Then the flow equations are established. Two regions are considered in the channel. The region near the center of the channel is called core flow region and the flow near the channel wall is called as porous flow region. Reynolds's number is defined as $\mathrm{Re} = \frac{\rho u d}{\mu}$ where ρ is the density of the blood in the channel and taken $1.06 \frac{g}{cm^3}$, u is the characteristic velocity of the flow $(\frac{mm}{s})$ and found by the solution of the equations in the channel, d is the diameter of channel, μ is the viscocity of the blood and taken 3.5 cP. Typical Reynold's number in micro channel is around 0.05. General mathematical formulations for the calculation of the velocities in both regions are derived. The mixed problem for one-dimensional diffusion equation with variable space operator is solved. A numerical code is written using Matlab software. The results of the solution will lead us to calculate the wall shear stress (WSS) and drag forces inside the geometry.

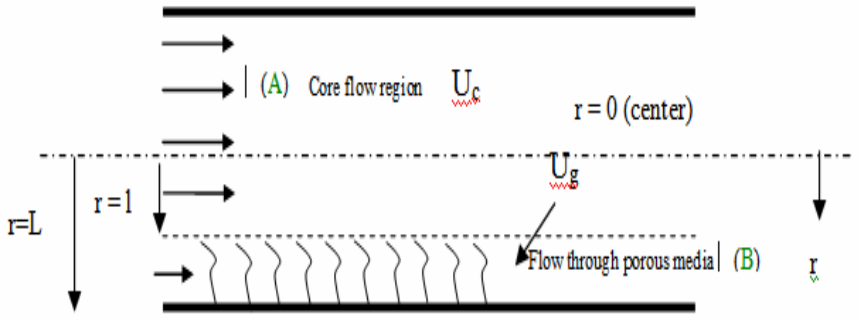

Figure 3. Schematic of Core (A) and Porous flow (B) regions inside capillary arteries.

Differential equations together with boundary and initial conditions are given for core and porous flow regions by equation (5.1) through equation (5.3) . Core flow region is defined through the center of capillary and porous flow region is through the glycocalyx.

Core flow region:

$$\frac{\partial u\left(t,x\right)}{\partial t}=\frac{\partial}{\partial x}\left(a\left(t,x\right)\frac{\partial u\left(t,x\right)}{\partial x}\right)+f\left(t,x\right),\ x\in\left(0,l\right),t\in\left(0,T\right). \tag{5.1}$$

Porous flow region:

$$\begin{aligned}\frac{\partial u\left(t,x\right)}{\partial t}&=\frac{\partial}{\partial x}\left(a\left(t,x\right)\frac{\partial u\left(t,x\right)}{\partial x}\right)+b\left(t,x\right)u\left(t,x\right)\\&+g\left(t,x\right),\ x\in\left(0,l\right),t\in\left(0,T\right).\end{aligned} \tag{5.2}$$

Initial and boundary conditions:

$$\begin{aligned}&u\left(0,x\right)=\varphi\left(x\right),\ x\in\left[0,L\right],\\&u_x(t,0)=0,u(t,L)=0,t\in[0,T],\\&u(t,l+)=u(t,l-),u_x(t,l+)=u_x(t,l-),t\in[0,T].\end{aligned} \tag{5.3}$$

where $a(t,x)$, $b(t,x)$, $f(t,x)$, $g(t,x)$ and $\varphi(x)$ are given sufficiently smooth functions and $a(t,x)\geqslant 0$. $a(t,x)$ is due to taking cylindrical coordinates in the system and defined as x. The function $b(t,x)$ is the ratio of viscosity to Darcy permeability which describes how densely the proteoglycans are packed. $f(t,x)$ and $g(t,x)$ are the pressure differences along the micro channels under unsteady fluid flow conditions in cylindrical coordinates.

The discretization of the problem is carried out in two steps. In the first step the grid spaces are defined as illustrated in Figure 4.

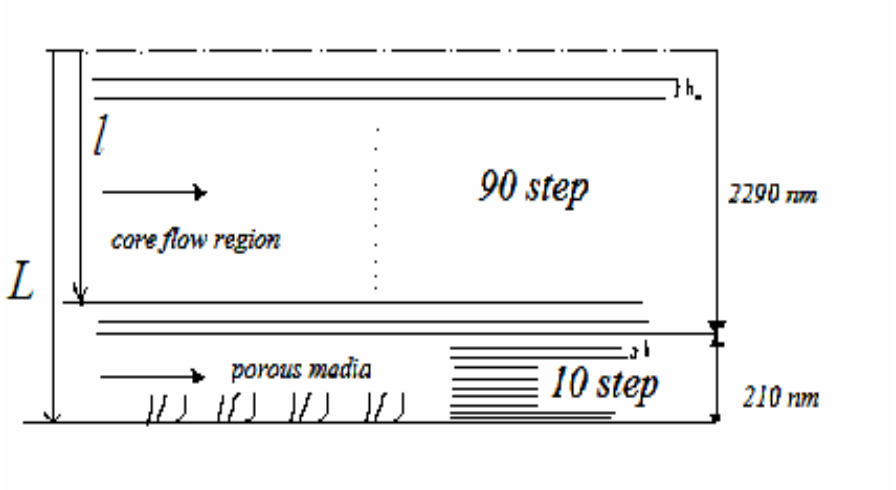

Figure 4. Grid spaces inside the Core and Porous regions in the capillary arteries.

In x-direction, we define two different step sizes h_0 and h for core flow and porous media regions for numerical calculations respectively. Finer grid size h in porous media defines to observe the velocity, drag force and WSS over the glycocalyx in detailed.

5.3. Results and Discussion

The flow field inside the capillary vascular system was solved using differential equations which are valid through the core and porous regions. Differential equations are discretized and solved using MATLAB software. A computer code was written to solve the algebraic equations. Velocity profiles for unsteady flow were given in Figure 5. First and second orders of accuracy approach were applied to the equations for the velocities. Time

dependent velocities are increasing inside the domain starting from the capillary wall.

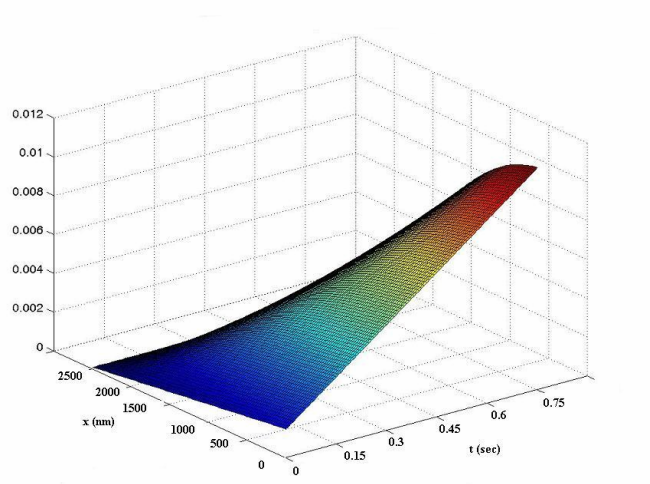

Figure 5. Unsteady velocity profiles.

Figure 6 illustrates the velocity profiles at some specific locations inside the core and porous regions. Velocity increases by time in the center of the capillary (x=0). While getting closer to the wall velocity change is not remarkably high by time. It becomes smooth through the period. Velocity is high near to the junction of core flow and flow through the glycocalyx. Then it becomes very small near to the wall. When the pressure or flow rate is increased inside the vessel, we observed fast change of flow speed and more blunt velocity profiles indicating the increased momentum transfer in the vertical direction to the flow direction.

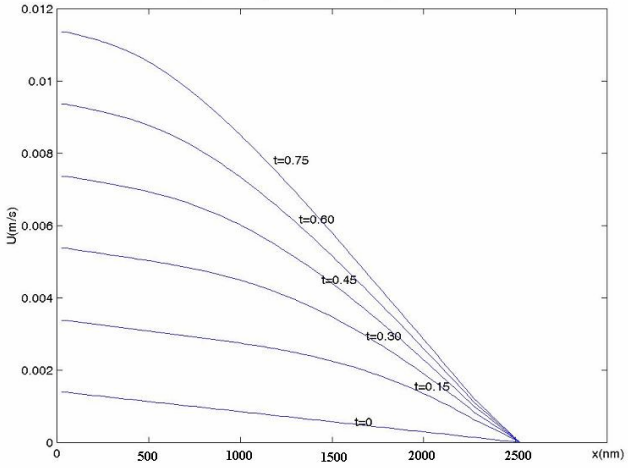

Figure 6. Velocity profiles at some specific locations inside the core and porous regions.

Drag forces inside the porous media or through the glycocalyx were shown in the Figure 7. The equation for drag force is $F_{drag} = \frac{\pi \mu u a^2}{c K_p}$ where K_p is Darcy permeability function and taken as $278.03 nm^2$, volume fraction of the proteoglycans c is taken 0.0252, a is the protein radius and taken as 5 nm. Drag force at the edge of the glycocalyx was found the smallest (0.2 10^{-7} pN) that is because of very small tip cross sectional area. Then the value increases along the glycocalyx upto the wall. The magnitude of the drag force is also increased by time.

The wall shear stresses $\left(WSS = \mu \frac{\Delta u}{\Delta r},\ \frac{\Delta u}{\Delta r} : velocity\ gradient\right)$ inside the glycocalyx were shown in Figure 8. At the beginning of the pulsatile flow the value of WSS value is higher near to the edge of the glycocalyx and inside the porous region. It gets smaller due to the lower velocity gradient. This is one of the effects of mechanotransduction which may be effective for biochemical signaling.

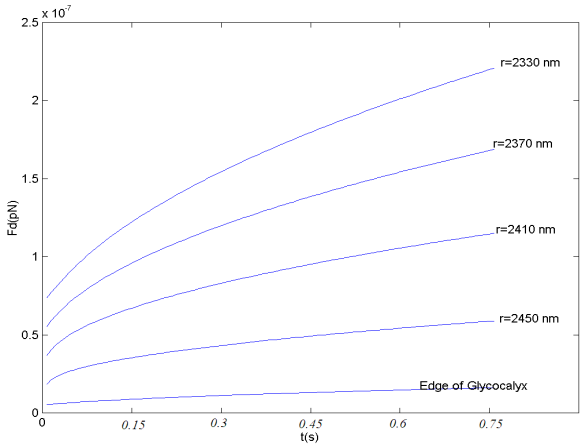

Figure 7. Drag Force changes inside the porous region.

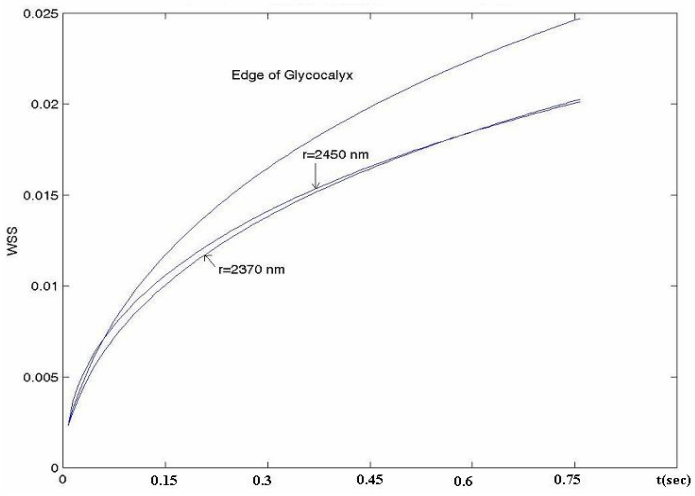

Figure 8. Wall shear stress distribution by time inside the core and porous flow regions.

CHAPTER 6

CONCLUSIONS

This work is devoted to study the stability of the difference schemes for the approximate solution of the partial differential equations with variable space operator. The following original results are obtained:

* First and second order of accuracy difference schemes for the approximate solution of the partial differential equations with variable space operator in a Hilbert space are presented.

* Theorems on the stability estimates for the solution of these differences schemes are established.

*The Matlab implementation of these differences schemes are generated.

* Theoretical statements for the solution of these difference schemes are supported by results of numerical examples.

* Constructed Matlab implementation is used to obtain the solution of the given application.

* Velocity profile is analyzed.

* Drag forces is calculated in both regions. Drag forces are found higher at the edge of the glycocalyx and decreased along them.

* Low WSS can be considered one of the causes of the atherosclerosis formation and biochemical signal activator. In vivo studies together with the modeling studies will give more detailed understanding of the flow phenomena inside capillary arteries.

CHAPTER 7

MATLAB PROGRAMMING

In this chapter, Matlab programs for first order of accuracy difference schemes for different h and h_0 and the biomechanical application are presented.

7.1. First order of Accuracy Difference Scheme

```
function firstorderaccuracy(N,M)

if nargin<1; N=20; M=20; end;

T=1 ; ML=13*M/20; a=1 ; q=1 ; h=0.01

ho=(pi-(h*(M-ML)))/ML; tau=T/N; l=ML*ho;

A=zeros(M+1,M+1) ;

for n=1:ML-1;

A(n+1,n)=-(a*(n-1)/ho); A(n+1,n+1)=(1/tau)+(a*(n-1)+(a*n))/ho ; A(n+1,n+2)=
-(a*n)/ho;

end;

for n=ML+1:M-1;

A(n+1,n)=-(l+(n-ML-1)*h)/h^2 ;

A(n+1,n+1)=(1/tau)+(2*l+(2*n-2*ML-1)*h)/h^2+q ;
```

```
A(n+1,n+2)= -(l+(n-ML)*h)/h^2 ;

end;

A(1,1)=1 ; A(1,2)=-1 ; A(ML+1,ML)=h ; A(ML+1,ML+1)=-h-ho ;

A(ML+1,ML+2)=ho ; A(M+1,N+1)=1 ;

P=zeros(M+1,M+1) ;

for n=2:ML; P(n,n)=-1/tau ; end;

for n=ML+2:M;  P(n,n)=-1/tau ; end;

fii=zeros(M+1,M+1) ;

for k=2:M+1;  fii(1,k)=0 ; fii(ML+1,k)=0 ; fii(M+1,k)=0 ;

for n=2:ML; t=(k-1)*tau; x=(n-1)*ho ; fii(n,k)=f(x,t);  end;

for n=ML+2:M; t=(k-1)*tau; x=ML*ho+(n-ML-1)*h ;

fii(n,k)=c(x,t);  end; end;

G=inv(A) ;

for n=1:ML ; U(n,1)=cos((n-1)*ho/2) ; end;

for n=ML+1:M+1 ; U(n,1)=cos((ML*ho+(n-ML-1)*h)/2) ; end;

for k=2:N+1 U(:,k)=G*fii(:,k)-G*P*U(:,k-1); end;
```

```
%'EXACT SOLUTION OF PDE' ;

for k=1:N+1; for j=1:ML+1;  t=(k-1)*tau; x=(j-1)*ho;

es(j,k) = exact(x,t); end;

for j=ML+2:M+1; t=(k-1)*tau; x=ML*ho+(j-ML-1)*h;

es(j,k) = exact(x,t); end; end;

% ABSOLUTE DIFFERENCES ;

absdiff=max(max(abs(es-U)))

% DIFFERENCE ANALYSIS ;

for k=1:N+1; for n=1:ML+1 ;

diff(k,n)=(abs(U(k,n)-es(k,n)))^2*h;

end;

for n=ML+2:M+1 ;

diff(k,n)=(abs(U(k,n)-es(k,n)))^2*h;

end; end;

for s=1:N+1; diffsum(s)=sum(diff(s,:)); end;

for s=1:N+1; kare(s)=diffsum(s)^0.5; end;
```

Err2=max(kare)

%GRAPH OF THE SOLUTION ;

figure; surf(U); title('first order accuracy for N=20 M=20');xlabel('t axis'); ylabel('x axis'); rotate3d ;

figure; surf(es); title('exact solution'); xlabel('t axis'); ylabel('x axis');rotate3d ;

%FUNCTIONS ;

function estx=exact(x,t); estx=exp(-t/2)*cos(x/2);

function ftx=f(x,t) ; ftx=exp(-t/2)/2*((x-2)/2*cos(x/2)+sin(x/2)) ;

function ctx=c(x,t); ctx=exp(-t/2)/2*((x+2)/2*cos(x/2)+sin(x/2));

7.2. Application

function application(N,M)

if nargin<1; N=100; M=100; end;

T=0.75 ; ML=9*M/10; a=1 ; q=1 ;

%h is the step size in porous mediada and ho is inside core flow region , tau is

% the time incrementation. Porous media has 10 nodes in x direction while

%core flow region has 90.Error analysis can be calculated when the exact solution is known.

```
h=0.021;  ho=(2.5-(h*(M-ML)))/ML;

tau=T/N;  l=ML*ho;

%l is the lenght of core flow region

A=zeros(M+1,M+1) ;

for n=1:ML-1;

A(n+1,n)=-a*((n-1)*ho)^2/(2*ho^2);

A(n+1,n+1)=(1/tau)+((a*((n-1)*ho)^2)+(a*(n*ho)^2))/(2*ho^2) ;

A(n+1,n+2)= -a*(n*ho)^2/(2*ho^2);

end;

for n=ML+1:M-1;

A(n+1,n)=-a*(l+(n-ML-1)*h)^2/(2*h^2) ;

A(n+1,n+1)=(1/tau)+a*((l+(n-ML-1)*h)^2+(l+(n-ML)*h)^2)/(2*h^2)+q ;

A(n+1,n+2)= -a*(l+(n-ML)*h)^2/(2*h^2) ;

end;

A(1,1)=1 ;A(1,2)=-1 ;  A(ML+1,ML)=h ;  A(ML+1,ML+1)=-h-ho ;

A(ML+1,ML+2)=ho ;  A(M+1,N+1)=1 ;
```

```
P=zeros(M+1,M+1) ;

for n=2:ML;  P(n,n)=-1/tau ;  end;

for n=ML+2:M;  P(n,n)=-1/tau ;  end;

fii=zeros(M+1,N+1) ;

for k=2:N+1;  fii(1,k)=0 ;  fii(ML+1,k)=0 ;  fii(M+1,k)=0 ;

for n=2:ML;  t=(k-1)*tau;x=(n-1)*ho ;fii(n,k)=f(x,t);  end;

for n=ML+2:M;t=(k-1)*tau;  x=ML*ho+(n-ML-1)*h ;  fii(n,k)=c(x,t);  end;  end;

G=inv(A) ;

for n=1:ML ;  U(n,1)=1.4-1.4*(n-1)/M;  end;

for n=ML+1:M+1 ;  U(n,1)=1.4-1.4*(n-1)/M;  end;

for k=2:N+1  U(:,k)=G*fii(:,k)-G*P*U(:,k-1);  end;

%ANALYZING U FOR CONSTANT X's INSIDE TWO REGIONS ;

for j=1:M+1;  UC1(j,1)=U(1,j);  UC2(j,1)=U(26,j);  UC3(j,1)=U(51,j);

UC4(j,1)=U(71,j);  UC5(j,1)=U(89,j);  UG1(j,1)=U(91,j);  UG2(j,1)=U(93,j);

UG3(j,1)=U(95,j);  UG4(j,1)=U(98,j);  UG5(j,1)=U(101,j);  end;

subplot(1,2,1);
```

```
plot(UC1); gtext('r=0'); xlabel('t(s)');ylabel('Uc(mm/s)');hold;

plot(UC2); gtext('r=0.06');  plot(UC3); gtext('r=0.13');

plot(UC4); gtext('r=0.18');  plot(UC5); gtext('r=0.22');

title('Figure 3.1.1 Time changes of velocity in core flow');

subplot(1,2,2);

plot(UG1); gtext('r=0.228');xlabel('t(s)'); ylabel('Ug(mn/s)');hold;

plot(UG2); gtext('r=0.23');  plot(UG3); gtext('r=0.237');

plot(UG4); gtext('r=0.243');  plot(UG5); gtext('r=0.25');

title('Figure 3.1.2 Time changes of velocity in porous media');

%ANALYZING U FOR CONSTANT T's;

for j=1:M+1;

T1(j,1)=U(j,1);  T2(j,1)=U(j,21);   T3(j,1)=U(j,41); T4(j,1)=U(j,61);

T5(j,1)=U(j,81);  T6(j,1)=U(j,101);  end;

figure;

plot(T1); gtext('t=0'); xlabel('x(nm)');ylabel('U(mn/s)');hold;

plot(T2); gtext('t=0.15');  plot(T3); gtext('t=0.30');
```

```
plot(T4); gtext('t=0.45');  plot(T5); gtext('t=0.60');

plot(T6); gtext('t=0.75');

title('Figure 3.2 Velocity changes for different time levels in whole region');

%ANALYZING U FOR T=0.45;

for j=1:(9*M/10)-3;  TL(j,1)=U(j,61);  end;

for j=(9*M/10)-3:(9*M/10)+3;  TNT(j-9*M/10+4,1)=U(j,61);  end;

for j=(9*M/10)+1:M+1;  TBB(j-9*M/10,1)=U(j,61);  end;

figure;

subplot(1,3,1);plot(TL); title('Velocity in lumen');

xlabel('x(nm)');ylabel('U(mn/s)');

subplot(1,3,2);plot(TNT); title('Velocity near tip');

xlabel('x(nm)');ylabel('U(mn/s)');

subplot(1,3,3);plot(TBB); title('Velocity in brush border');

xlabel('x(nm)');ylabel('U(mn/s)');

%WALL SHEAR STRESS;

W=zeros(M+1,N+1);
```

```
for k=1:ML-2;  for n=1:N+1;

W(k+1,n)=(-U(k+1,n)+U(k,n))/ho;

end; end;

for k=ML-1:M;  for n=1:N+1;

W(k+1,n)=(-U(k+1,n)+U(k,n))/h;

end; end;

mu=0.0035;  WSS=mu*W;  for j=1:M+1;

W1(j,1)=WSS(91,j);  W2(j,1)=WSS(93,j);

W3(j,1)=WSS(95,j);  W4(j,1)=WSS(97,j);

W5(j,1)=WSS(99,j);

figure;

plot(W1); gtext('Edge of Glycocalyx');xlabel('t');

ylabel('WSS');hold;

plot(W2); gtext('r=2330 nm');  plot(W3); gtext('r=2370 nm');

plot(W4); gtext('r=2410 nm');  plot(W5); gtext('r=2450 nm');

title('Figure 3.3 Wall shear stress changes inside porous media');
```

```
%DRAG FORCE AT THE END OF GLYCOCALYX;

Kp=278.03;  e=0.0252;  ap=0.01;

for k=1:N+1;

Fd1(1,k)=pi*mu*U(91,k)*ap^2/e/Kp/4;

Fd11(1,k)=pi*mu*U(92,k)*ap*2/e/Kp*0.021;

Fd2(1,k)=pi*mu*U(93,k)*ap*2/e/Kp*0.021;

Fd21(1,k)=pi*mu*U(94,k)*ap*2/e/Kp*0.021;

Fd3(1,k)=pi*mu*U(95,k)*ap*2/e/Kp*0.021;

Fd31(1,k)=pi*mu*U(96,k)*ap*2/e/Kp*0.021;

Fd4(1,k)=pi*mu*U(97,k)*ap*2/e/Kp*0.021;

Fd41(1,k)=pi*mu*U(98,k)*ap*2/e/Kp*0.021;

Fd5(1,k)=pi*mu*U(99,k)*ap*2/e/Kp*0.021;

end;

figure;

plot(Fd1); gtext('Edge of Glycocalyx');xlabel('t(s)');

ylabel('Fd(pN)');hold;
```

```
plot(Fd2); gtext('r=2330 nm');  plot(Fd3); gtext('r=2370 nm');

plot(Fd4); gtext('r=2410 nm');  plot(Fd5); gtext('r=2450 nm');

title('Figure 3.3 Drag Force changes inside porous media');

%RELATION BETWEEN DRAG COEFFICIENT (F/(mu*U)) AND OPEN GAP

ap=10;

for delta=40:200;

c2(delta)=pi*2/3^0.5/(2+delta/ap)^2;

Kp2(delta)=ap^2*(log(c2(delta)^-0.5)-0.745+c2(delta)-1/4*c2(delta)^2)/(4*c2(delta));

DC(delta)=pi*ap^2/e/Kp2(delta);

end;

figure;

plot(DC); title('Relation between open gap and drag coefficient');

xlabel('delta'); ylabel('Drag Coefficient');hold;

% PERCENT OF DRAG FORCE-RADIAL POSITION ;

TFD=Fd1+Fd11+Fd2+Fd21+Fd3+Fd31+Fd4+Fd41+Fd5;

TFDRP(1)=0;
```

```
TFDRP(2)=Fd1(1,50)/TFD(1,50);

TFDRP(3)=TFDRP(2)+Fd11(1,50)/TFD(1,50);

TFDRP(4)=TFDRP(3)+Fd2(1,50)/TFD(1,50);

TFDRP(5)=TFDRP(4)+Fd21(1,50)/TFD(1,50);

TFDRP(6)=TFDRP(5)+Fd3(1,50)/TFD(1,50);

TFDRP(7)=TFDRP(6)+Fd31(1,50)/TFD(1,50);

TFDRP(8)=TFDRP(7)+Fd4(1,50)/TFD(1,50);

TFDRP(9)=TFDRP(8)+Fd41(1,50)/TFD(1,50);

TFDRP(10)=TFDRP(9)+Fd5(1,50)/TFD(1,50);

figure;

plot(TFDRP); xlabel('dimensionless radial position');

ylabel('percent of total drag force');hold;

%GRAPH OF THE SOLUTION ;

figure; surf(U); title('first order of accuracy approach for velocity');

xlabel('t(100 step-0.75 s) '); ylabel('x(100 step-2500 nm)');rotate3d ;

%figure; surf(es); title('exact solution'); xlabel('t axis'); ylabel('x axis');rotate3d ;
```

```
figure; surf(WSS); title('wall shear stress'); xlabel('t axis'); ylabel('x axis');

rotate3d ;

%FUNCTIONS ;

function ftx=f(x,t) ; ftx=0.0133 ;

function ctx=c(x,t); ctx=0.0133;
```

REFERENCES

Luft J. H.,"Fine Structure of capillary and endocapillary layer as revealed by ruthenium red", *Proc. Fed. Am. Soc. Expl Biol.,* Vol.25, pp.1773-1783,1965.

Vink H. and Duling B. R.,"Identification of distinct luminal domains for macromolecules, erythrocytes, and leukocytes within mammalian capillaries", *Circulation Research,* Vol.79, no.3, pp.581-589,1996.

Michel C.C., "Starling: the formulation of his hypothesis of microvascular fluid exchange and its significance after 100 years", *Experimental Physiology,* Vol.82, pp.1-30,1997.

Weinbaum S.," Whitaker distinguished lecture: Models to solve mysteries in biomechanics at the cellular level; A new view of fiber matrix layers", *Annals of Biomedical Engineering,*Vol.26, no.4, pp.627-643, 1998.

Hu X. and Weinbaum S., "A new view of Starling's hypothesis at the microstructural level", *Microvascular Research,*Vol.58, no.3, pp.281-304, 1999.

Hu X.,Adamson R.H., Liu B., "Curry F.E. and WeinbaumS., Starling forces that oppose filtration after tissue oncotic pressure is increased", *The American Journal of Physiology - Heart and Circulatory Physiology,* Vol.279**,** no.4, pp.1724-1736, 2000.

Feng J. and Weinbaum S., "Lubrication theory in highly compressible porous media: the mechanics of skiing, from red cells to humans", *Journal of Fluid Mechanics,* Vol.422 , pp.281-317, 2000.

Secomb T.W., Hsu R. and Pries A.R., "Motion of red blood cells in a capillary with an endothelial surface layer: effect of flow velocity", *American Journal Of Physiology-*

Heart And Circulatory Physiology, Vol.281 , no.2, pp.H629-H636, 2001.

Damiano E.R., "The Effect of the Endothelial-Cell Glycocalyx on the Motion of Red Blood Cells through Capillaries", *Microvascular Research,* Vol.55, no.1, pp.77-91, 1998.

Zhao Y.H., Chien S. and Weinbaum S., "Dynamic contact forces on leukocyte microvilli and their penetration of the endothelial glycocalyx", *Biophysical Journal,* Vol.80, no.3, pp.1124-1140, 2001.

Davies P.F., Flow-Mediated Endothelial Mechanotransduction, *Physiological Reviews,* **75**, no.3, 519-560, 1995.

Secomb T.W., Hsu R. and Pries A.R.,"A model for red blood cell motion in glycocalyx-lined capillaries", *American Journal Of Physiology-Heart And Circulatory Physiology,* Vol.274, no.3, pp.H1016-H1022, 1998.

Secomb T.W., Hsu R. and Pries A.R.,"Effect of the endothelial surface layer on transmission of fluid shear stress to endothelial cells", *Biorheology,* Vol.38, no.2-3, pp.143-150, 2001.

Dehghan M., "On the numerical solution of the diffusion equation with a nonlocal boundary condition", *Mathematical Problems in Engineering,* Vol.2003, no.2, pp.81-92, 2003.

Cannon J. R., Perez Esteva S. and van der Hoek J., "A Galerkin procedure for the diffiusion equation subject to the specification of mass", *SIAM J. Numerical Analysis.* Vol.24, no.3, pp.499-515, 1987.

Gordeziani N., Natani P. and Ricci P.E., "Finite-difference methods for solution of nonlocal boundary value problems", *Computers and Mathematics with Applications,* Vol.50, pp.1333-1344, 2005.

Ashyralyev A. and Ozdemir Y., "Stability of difference schemes for hyperbolic-parabolic equations", *Computers and Mathematics with Applications,* Vol.50, no.8-9, pp.1443-1476, 2005.

Squire J.M., Chew M., Nneji G., Neal C., Barry J. and Michel C., "Quasi-periodic substructure in the microvessel endothelial glycocalyx: A possible explanation for molecular filtering?", *Journal of Structural Biology,* Vol.136, no.3, pp.239-255, 2001.

Ashyralyev A., Erdogan A.S. and Arslan N.,"On the numerical solution of the diffusion equation with variable space operator", *Applied Mathemetics and Computation,* Vol.189, no.1, pp.682-689,2007.

Loth F., Fischer P.F., Arslan N., Bertram C.D., Lee S.E., Royston T.J., Shaalan W.E. and Bassiouny H.S., "Transitional flow at the venous anastomosis of an arteriovenous graft: Potential activation of the ERK1/2 mechanotransduction pathway", *Journal of Biomechanical Engineering ,* Vol.125, pp.49-61, 2003.

Ashyralyev A. and Sobolevskii P.E., *New Difference Schemes for Partial Differential Equations,* Birkhäuser Verlag, Basel, Boston, Berlin, Operator Theory and Appl., 2004, Vol.148, 443p.

Ashiraliev A. and Sobolevskii P.E.," Differential schemes of high order of accuracy for parabolic equations with variable coefficients", *Dopovidi Akademii Nauk Ukrainskoi RSR Seriya A-Fiziko-Matematichni ta Technichni Nauki,* no. 6, pp.3–7, 1988.(Russian).

Ashyralyev A., "An estimation of the convergence for the solution of modified Crank-Nicholson difference schemes for parabolic equations with nonsmooth initial data", *Izv. Akad. Nauk Turkmen, SSR Ser. Fiz-Tekhn. Khim. Geol. Nauk*, no.1, pp.3-8, 1989.(Russian)

Luskin M. and Rannacher R., "On the smoothing property of the Crank-Nicholson

scheme",*Appl. Anal.,* Vol.14, pp.117-135, 1982.

Rannacher R., "Discretization of the heat equation with singular initial data", *Z. Angew. Math. Mech.,* Vol.62, no.5, pp.346-348,1982.